

AD-A168 484

SPREAD SPECTRUM MOBILE RADIO COMMUNICATIONS

under contract

AFOSR-82-0309

with

Air Force Office of Scientific Research
Bolling Air Force Base
Washington, D.C.

DTIC
SELECTED
JUN 06 1986
S D D

Electrical Engineering Department
School of Engineering and Applied Science
Southern Methodist University

Dallas, Texas 75275

Approved for public release;
distribution unlimited.



DTIC FILE COPY

②

SPREAD SPECTRUM MOBILE RADIO COMMUNICATIONS

under contract

AFOSR-82-0309

with

Air Force Office of Scientific Research
Bolling Air Force Base
Washington, D.C.

INTERIM SCIENTIFIC REPORT

September 1, 1984

March 31, 1986

S.C. GUPTA, PRINCIPAL INVESTIGATOR

DTIC
ELECTE
JUN 06 1986
S D D

Electrical Engineering Department
School of Engineering and Applied Science
Southern Methodist University

Dallas, Texas 75275



DISTRIBUTION STATEMENT A

Approved for public release
Distribution Unlimited

REPORT DOCUMENTATION PAGE		READ INSTRUCTIONS BEFORE COMPLETING FORM	
1. REPORT NUMBER AFOSR-TR- 86 0323		2. GOVT ACCESSION NO. ADA 168484	
4. TITLE (and Subtitle) Spread Spectrum Mobile Radio Communications		3. RECIPIENT'S CATALOG NUMBER	
7. AUTHOR(s) S.C. Gupta		5. TYPE OF REPORT & PERIOD COVERED Interim Scientific Report Sept. 1, 1984 - March 31, 1986	
9. PERFORMING ORGANIZATION NAME AND ADDRESS Electrical Engineering Department Southern Methodist University Dallas, Texas		6. PERFORMING ORG. REPORT NUMBER	
11. CONTROLLING OFFICE NAME AND ADDRESS AFOSR/NE Building 410 Bolling AFB, DC 20332-6448		8. CONTRACT OR GRANT NUMBER(s) AFOSR #82-0309	
14. MONITORING AGENCY NAME & ADDRESS (if different from Controlling Office)		10. PROGRAM ELEMENT, PROJECT, TASK AREA & WORK UNIT NUMBERS <i>11-21</i> 3305 B3	
15. SECURITY CLASS. (of this report) <i>Unclass</i>		12. REPORT DATE March 31, 1986	
16. DISTRIBUTION STATEMENT (of this Report) Approved for public release; distribution unlimited.		13. NUMBER OF PAGES	
17. DISTRIBUTION STATEMENT (of abstract entered in Block 20, if different from Report)		15a. DECLASSIFICATION/DOWNGRADING SCHEDULE	
18. SUPPLEMENTARY NOTES			
19. KEY WORDS (Continue on reverse side if necessary and identify by block number) Spread Spectrum Mobile Packet Radio Network Carrier Sense Multiple Access Spectrally Efficient Modulation Speech Transmission			
20. ABSTRACT (Continue on reverse side if necessary and identify by block number) In this report we present some additional results on the performance of carrier sense multiple access (CSMA) protocol for mobile packet radio networks (MPRNET). This is followed by a review of bandwidth efficient digital modulation for mobile radios and some results on a speech transmission scheme and an analysis of mismatched continuous phase FSK (CPFSK) receivers. (Continued on back)			

Carrier sense multiple access protocol has been analyzed in detail for mobile radio channel. Throughput and delay expression are derived to include the effects of fading. The performance degradation due to hidden terminal problems is analyzed. This is followed by an evaluation of the performance of CSMA with collision detection (CSMA-CD) for FH-FSK spread spectrum mobile packet radio networks.

A class of spectrally efficient modulation has been reviewed for application to mobile radio systems. A speech transmission scheme using DPCM coding and these spectrally efficient modulation is seen to compete well with existing schemes.

Mismatched CPFSK receivers have been analyzed to understand how time and phase synchronization errors influence the performance. A set of curves is provided to demonstrate the degradation due to imperfect carrier phase or symbol time synchronization error for both low and high SNR.

SUMMARY

In this report we present some additional results on the performance of carrier sense multiple access (CSMA) protocol for mobile packet radio networks (MPRNET). This is followed by a review of bandwidth efficient digital modulation for mobile radios and some results on a speech transmission scheme and an analysis of mismatched continuous phase FSK (CPFSK) receivers.

Carrier sense multiple access protocol has been analyzed in detail for mobile radio channel. Throughput and delay expression are derived to include the effects of fading. The performance degradation due to hidden terminal problems is analyzed. This is followed by an evaluation of the performance of CSMA with collision detection (CSMA-CD) for FH-FSK spread spectrum mobile packet radio networks.

A class of spectrally efficient modulation has been reviewed for application to mobile radio systems. A speech transmission scheme using DPCM coding and these spectrally efficient modulation is seen to compete with existing schemes.

Mismatched CPFSK receivers have been analyzed to understand how time and phase synchronization errors influence the performance. A set of curves is provided to demonstrate the degradation due to imperfect carrier phase or symbol time synchronization error for both low and high SNR. 7

AIR FORCE RESEARCH AND DEVELOPMENT COMMAND
NOTICE
TECHNICAL REPORT
CDD
DISTRIBUTION STATEMENT
MILITARY
Chief, Technical Information Division

TABLE OF CONTENTS

- I. Applications of Packet Switching Mobile Radio Communications
 - 1.1 Introduction
 - 1.2 Mobile Packet Radio Channel Characteristics
 - 1.3 Model and Protocol Description

- II. Carrier Sense Multiple Access for Mobile Packet Radio Channels
 - 2.1 Channel Throughput and Packet Delay
 - 2.2 Probability of Block Error
 - 2.3 System Performance
 - 2.4 Probability of Block Error in Fast Fading
 - 2.5 Summary and Discussion

- III. Performance Degradation Due to Hidden Terminal Problem in CSMA for Mobile Packet Radio Channels
 - 3.1 Non-Persistent CSMA with Hidden Terminals
 - 3.2 Dynamic Block Error Rate
 - 3.3 System Performance
 - 3.4 Summary and Discussion

- IV. CSMA with Collision Detection for FH/FSK Spread Spectrum Mobile Packet Radio Networks
 - 4.1 Introduction
 - 4.2 Dynamic Block Error Probability
 - 4.3 Numerical Results and System Performance
 - 4.4 Conclusions

- V. Bandwidth Efficient Digital Modulation for Mobile Radios
 - 5.1 Introduction
 - 5.2 Transmitter and Receiver Principles
 - 5.3 Performance
 - 5.4 Discussions

- VI. Speech Transmission using DPCM Coding, Partial Response CPM, and Diversity
 - 6.1 Introduction
 - 6.2 Fading and Diversity Combining
 - 6.3 Source Coders
 - 6.4 Performance Evaluation
 - 6.5 Discussion and Conclusions



Accession For	
NTIS CRA&I	<input checked="" type="checkbox"/>
DTIC TAB	<input type="checkbox"/>
Unannounced	<input type="checkbox"/>
Justification	
By _____	
Distribution / _____	
Availability Codes	
Dist	Avail and/or Special
A-1	

VII. Performance Degradation due to Receiver Mismatch in Binary
Continuous-Phase Modulation Systems

- 7.1 Introduction
- 7.2 Receiver Structure
- 7.3 Performance of Mismatched Receiver
- 7.4 Conclusions

CHAPTER I

APPLICATIONS OF PACKET SWITCHING TO MOBILE RADIO COMMUNICATIONS

The need to provide computer network access to mobile terminals and computer communications in the mobile environment has stimulated and motivated the current developments in this area. Packet radio technology has developed over the past decade in response to the need for real-time, interactive communications among mobile users and shared computer resources. In computer communication systems we have a great need for sharing expensive resources among a collection of high peak-to-average (i.e. bursty) users. Packet radio networks provide an effective way to interconnect fixed and mobile computer resources. This report presents the performance evaluation of various channel access protocols for a mobile packet radio network link.

1.1 INTRODUCTION

A mobile computer communication network can generally be defined by the following features: its host computers and terminals, communication processors, topological layout, communication equipment and transmission media, switching technique, mobile unit and protocol design [1]. These features are chosen to accomplish the function of the network subject to specified performance requirements. The performance measures most commonly quoted include message delay, message throughput, error rate, reliability, and cost. When mobile operations are involved, the measurements indicate temporary degradation in the performance, affecting both throughput and delay. By proper selection of the dominant network protocol parameters, the degradation can be substantially reduced. Improved performance under mobile operations is needed for all traffic types, to reduce the load on the radio channel and improve overall network performance. Several methods for such improvements have been discussed in [2].

The first analysis of packet radio performance assumed that packet collisions were the major cause for loss of a packet and subsequent retransmission. More recently, efforts to design packet radio systems to operate over degraded channels have been undertaken. The channel throughput and packet delay, the two primary performance criteria in computer communications, have been extensively studied for basic system concepts such as pure ALOHA, slotted ALOHA, and CSMA [3,4]. However, we need to consider the effect of link errors due to noise and fading too. In the absence of fading the noiseless assumption is quite good, but on a fading channel the signal-to-noise ratio becomes a critical parameter. The approach here is to model the problem under fading conditions and develop a protocol for evaluating the performance of the mobile packet radio network in terms of packet error rate, packet delay, throughput and average number of packets retransmitted per cycle, as a function of packet transmission rate, packet size, the number of packets transmitted per cycle and vehicle speed.

1.2 MOBILE PACKET RADIO CHANNEL CHARACTERISTICS

A potential application of packet radio involves mobile users in an urban environment. Here, because of signal reflections from buildings and other structures, the signal arriving at the receiver consists of the sum of randomly delayed versions of the transmitted signal due to multipath. Hence, the signal amplitude should be Rayleigh distributed, and this has been found in practice [5]. Of course, if for some reason, packet radio were applied to HF or troposcatter systems, the Rayleigh, Rician and Nakagami-m models would also be applicable.

The mobile packet radio channel environment can be characterized as follows:

- a. Time-varying channel
- b. Short-term characteristics - fading of the received signal envelope due to multipath propagation. Statistics of the received signal envelope is Rayleigh distributed and phase of the received signal is uniformly distributed.
- c. Long-term characteristics - shadowing of the received signal envelope due to buildings, hills, trees, etc. Local mean of the received signal envelope obeys log-normal distribution.
- d. Attenuation of the signal with distance - signal power varies inversely as the M^{th} power of distance ($3 < M < 4$).
- e. Doppler effect due to vehicle motion.
- f. Ignition and other vehicular noise.

Atmospheric optical paths, tropospheric and ionospheric channels and intra-urban mobile radio channels all suffer from signal fading, a phenomenon produced by partial reinforcement or cancellation among the signals which reach the receiver by different paths. Although the traditional remedy has been diversity transmission, a considerably more effective alternative exists. The receiver can monitor the instantaneous path gain and send back requests for the transmitter to stop sending when the signal is weak and to resume when the signal is strong in order to compensate for the fading process. This and other adaptive methods have been the objective of study for some years, and it has been established that they provide substantially better performance than diversity systems.

1.3 MODEL AND PROTOCOL DESCRIPTION

Experiments in urban areas have shown that noise impulses occur every few milliseconds in both the UHF and L bands, principally due to automobile ignition noise. A packet has a very high probability of encountering one or

two bits per packet, therefore some form of error correction is required [6], if essentially an error-free performance for computer communication is desired. A target objective of no more than one undetected packet error per 10^6 packets is desired assuming 128 bit packets, a 100 K-bit/sec. data rate and 100 percent occupancy.

In the ground-based mobile packet radio network performance degradation occurs due to transmission errors resulting from packet collisions, noise, fading, and probably shadowing too. The present model assumes that transmission errors are caused only by fading i.e. errors due to other sources of noise and interference are not considered.

Packet radio techniques are used for communications between mobile terminals and computer networks. In these techniques, a message is decomposed into a number of packets which are transmitted individually to one or more destinations where they are assembled to reconstruct the original message. An overhead message is attached to each packet. The overhead message contains information about the addresses of the originating source and the destination, routing information and check-sum bits for error detection [7,8].

The transmission of packets is conducted in cycles. Each cycle consists of the transmission of N consecutive packets plus a short time interval to allow for the reception of the acknowledgement message.

In any communication system, and in particular, a computer communication system, it is essential to have a set of well-designed basic control procedures to insure efficient, correct, and smooth transfer of information in the system.

We describe and analyze a protocol derived from the "stop-and-wait" control procedures [8]. According to this protocol, the transmitting unit sends one packet of data at a time and waits for an acknowledgement (ACK) from the receiving unit before proceeding. If the transmitting unit does not

receive an ACK after a certain time-out period, the same packet is retransmitted. This operation is repeated for a predefined number of times until the ACK is received. However, when the channel is unreliable, the transmitting unit may be instructed to give up retransmitting the packet. We assume that the acknowledgement traffic is carried by a separate channel and is received reliably. In this protocol, the packet transmission is conducted in cycles. Each cycle represents the transmission of N packets plus an ACK time-out period. The ACK message informs the sending unit of the first packet that was found in error such that in the following cycle this packet and the following ones are to be retransmitted along with some new packets. Based on an estimation of the signal level at the receiving location or on the frequency of packet errors, the number of packets per cycle, N , can be adjusted.

An important parameter of the algorithm described above is the number of packets per cycle, N . For a certain set of system parameters, N can be adjusted to provide the minimum delay per message. More important is the fact that N can be made adaptive to the status of the channel to achieve minimum delay in the ever changing environment of the mobile system [5]. We notice that the case when $N=1$ represents the well-known stop-and-wait strategy, and the algorithm described above is a generalization of this strategy.

CHAPTER II

CARRIER SENSE MULTIPLE ACCESS FOR MOBILE PACKET RADIO CHANNELS

In this chapter we consider the performance of nonpersistent CSMA protocol for the mobile packet radio channel. The channel throughput and packet delay expressions are derived to include the effects of a fading additive white Gaussian noise channel. The average probability of block error for slow non-selective Rayleigh fading is derived for the noncoherent binary modulation scheme. The closed form expressions for the system performance parameters, throughput and delay, are obtained for the nonpersistent CSMA channel with noncoherent frequency shift keyed (MFSK) data transmission technique. We study the effect on these performance of various system parameters such as offered channel traffic, propagation delay, channel capacity and the signal-to-noise power ratio.

2.1 CHANNEL THROUGHPUT AND PACKET DELAY

The channel throughput and packet delay of packet radio channels have been determined for basic system concepts such as pure-ALOHA, slotted-ALOHA, and carrier sense multiple access (CSMA) [3 - 9]. However, none of these earlier analyses includes the effect of link errors due to noise and fading. For the mobile packet radio channel we need to modify the fundamental throughput-delay analysis, as the assumptions of nonfading, noiseless channel is no more good.

The channel throughput, S , is defined as the average number of packets successfully transmitted in an interval T seconds long where T is the packet duration. We have assumed that each packet is of constant length for all users. The parameter G is defined as the total 'offered' traffic rate on the channel. The ratio S/G equals the average percentage of packets transmitted that are successfully received, that is, it is probability of success on the first packet transmission, P_0 . Also, P_0 is equivalent to the probability that no packets are lost on the first transmission which for Poisson distributed packet transmissions are given by [3, 9]:

$$P_0 = \frac{S}{G} = \frac{e^{-2G}}{G(1 - 2e^{-2G}) + e^{-2G}} \quad (2.1)$$

This implies,

$$S = \frac{G e^{-2G}}{G(1 - 2e^{-2G}) + e^{-2G}} \quad (2.2)$$

for the nonpersistent CSMA channel throughput. Here, parameter a is the ratio of propagation delay (τ) to packet transmission time (T).

If the acknowledgement channel is error-free but the packet channel is fading, then the probability of success on the first packet transmission is:

$$P_S = \frac{S}{G} = \left(\frac{e^{-aG}}{G(1+2a) + e^{-aG}} \right) [1 - P_{pe}] \quad (2.3)$$

where P_{pe} is the probability that a packet is not accepted by the central receiving facility due to noise errors. Therefore,

$$S = \left(\frac{Ge^{-aG}}{G(1+2a) + e^{-aG}} \right) [1 - P_{pe}] \quad (2.4)$$

We assume here that all packet collisions result in lost packets. For a collision between a faded and a nonfaded packet, the nonfaded packet might not be lost. Hence (2.4) gives a lower bound on S .

If the acknowledgement channel is also fading, then acknowledgements can potentially arrive at the user receiver in error. Since each user must be able to positively identify his own acknowledgements, we assume that error detection coding is also utilized on acknowledgements and that perfect reception is required. Hence, errored acknowledgements will result in unnecessary packet transmissions. Based on the same reasoning as before, throughput equation for fading channel can be written as,

$$S = \left(\frac{Ge^{-aG}}{G(1+s) + e^{-aG}} \right) (1 - P_{pe}) (1 - P_{ae}) \quad (2.5)$$

The average packet delay, D , is defined as the average time (measured in packet lengths) between the beginning of the original user packet transmission and the beginning of the receipt of the acknowledgement from the central receiving facility. We assume that the two-way propagation delay equals R packet lengths and that the packet retransmission times are selected from a uniform distribution of delays ranging from one to K packet lengths. Then the average packet delay is given by [3, 10],

$$D = R + 1 + E \left(R + \frac{K+1}{2} \right) \quad (2.6)$$

where E is the average number of retransmissions per packet.

For noiseless channels

$$E = \frac{G}{S} - 1 = \left(\frac{G(1-2a) - e^{-aG}}{\exp(-aG)} - 1 \right) = [Ge^{aG}(1-2a)] \quad (2.7)$$

and the average packet delay is,

$$D \approx R + 1 + [Ge^{aG}(1+2a) \left(R + \frac{K+1}{2} \right)] \quad (2.8)$$

This expression for the delay is an approximation, even though (2.6) is exact, because the expression relating S and G assumes a very large average retransmission delay. However, (2.8) can be considered a good approximation for the exact expression for average packet delay even when K is as small as five [10].

To include the effects of fading, we need only modify E. Again assuming large K, the average number of transmissions per packet is, from (2.5),

$$\frac{G}{S} = \left(\frac{G(1-2a) - e^{-2G}}{e^{-2G}} \right) \frac{1}{(1 - P_{pe})(1 - P_{ae})} \quad (2.9)$$

Hence, the average number of retransmissions per packet is

$$R = \frac{G}{S} - 1 = \left[\left(\frac{G(1-2a) - e^{-2G}}{e^{-2G}} \right) \frac{1}{(1 - P_{pe})(1 - P_{ae})} - 1 \right] \quad (2.10)$$

Using (2.10) into (2.6) yields the average packet delay in fading,

$$D = R + 1 = \left[\left(\frac{G(1-2a) - e^{-2G}}{e^{-2G}} \right) \frac{1}{(1 - P_{pe})(1 - P_{ae})} - 1 \right] \left(R + \frac{K-1}{2} \right) \quad \dots (2.11)$$

where a is the normalized propagation delay.

2.2 PROBABILITY OF BLOCK ERROR

Consider a block of length N bits corresponding to either a packet or an acknowledgement. We assume that the communication system employs a digital modulation/demodulation scheme which produces independent bit errors with probability $\epsilon(\rho)$ where ρ is the bit energy-to-noise density ratio. The probability of block error, P_{be} , is the probability of at least one bit error in the block and is given by,

$$\begin{aligned} P_{be} &= \text{Prob}(\text{at least one error}) \\ &= 1 - \text{Prob}(\text{all bits received correctly}) \\ &= 1 - [1 - \epsilon(\rho)]^N \end{aligned} \quad (2.12)$$

Assuming constant ρ over the block length, the probability of block error averaged over the fading signal level is given by,

$$\begin{aligned} \bar{P}_{be} &= \int_0^{\infty} g(\rho) f(\rho) d\rho \\ &= \int_0^{\infty} [1 - (1 - \epsilon(\rho))^N] f(\rho) d\rho \end{aligned} \quad (2.13)$$

where $f(\rho)$ is the probability density function of ρ .

For the case of Rayleigh fading the signal power has an exponential probability density function [11]. Hence, ρ is also exponentially distributed and,

$$f(\rho) = \frac{1}{\bar{\rho}} \exp\left(-\frac{\rho}{\bar{\rho}}\right), \quad \rho \geq 0 \quad (2.14)$$

where $\bar{\rho}$ is the average value of ρ .

For the noncoherent modulation technique subject to additive white Gaussian noise, the bit error probability function is given by [11],

$$\epsilon(\rho) = c \exp(-b\rho) \quad (2.15)$$

For noncoherent FSK, $c = \frac{1}{2}$, $b = \frac{1}{\bar{\rho}}$. The average probability of block error can be determined in closed form.

Substituting (2.15) and (2.14) into (2.13) yields,

$$\bar{P}_{be} = \frac{1}{\bar{\rho}} \int_0^{\infty} [1 - (1 - c e^{-b\rho})^N] e^{-\rho/\bar{\rho}} d\rho$$

This expression simplifies to give exact expression for the average probability of block error,

$$\bar{P}_{be} = 1 - \frac{c^{-1/\bar{\rho}\beta}}{\bar{\rho}\beta} E_c\left(\frac{1}{\bar{\rho}\beta}, N-1\right) \quad (2.16)$$

where $E_x(a, b)$ is the incomplete Beta function [12]. Also,

$$\bar{P}_{be} = 1 - {}_2F_1\left(\frac{1}{\bar{\rho}\beta}, -N; 1 - \frac{1}{\bar{\rho}\beta}; c\right) \quad (2.17)$$

where, ${}_2F_1(a, b; c; x)$ is the hypergeometric function [12]. The incomplete Beta function and hypergeometric function can be evaluated by numerical methods.

The series representation for the hypergeometric function [12] is useful for obtaining exact results for \bar{P}_{be} , for small integer values of N . We obtain,

$$\bar{P}_{be} = \sum_{n=0}^N (-1)^{n-1} \binom{N}{n} \frac{c^n}{1 - \bar{\rho}\beta c} \quad (2.18)$$

There are some interesting asymptotic results for the average probability of block error \bar{P}_{be} , given by equations (2.17) or (2.18).

(a) For, $\bar{\rho}\beta \gg 1$, (2.18) becomes

$$\bar{P}_{be} \approx \frac{1}{\bar{\rho}\beta} \sum_{n=1}^N (-1)^{n-1} \binom{N}{n} \frac{c^n}{n} = \frac{\rho_0}{\bar{\rho}} \quad (2.19)$$

where we define

$$\rho_0 \triangleq \int_0^{\infty} [1 - (1 - ce^{-\beta\rho})^N] d\rho \triangleq \int_0^{\infty} g(\rho) d\rho \quad (\text{see})$$

$$\rho_0 \triangleq \frac{1}{\bar{\rho}} \sum_{n=1}^N (-1)^{n-1} \binom{N}{n} \frac{c^n}{n} \quad (2.20)$$

The series for ρ_0 can be transformed into a series with nonalternating, monotonically decreasing terms which is more convenient for computation than (2.20). Based on series results in [13, 14] we obtain,

$$\rho_0 = \frac{1}{\beta} \sum_{n=1}^N \frac{1 - (1-\alpha)^n}{n} \quad (2.21)$$

(b) If $N \gg 1$, asymptotic results can be applied to equation (2.21). We have [14],

$$\sum_{n=1}^N \frac{1}{n} = \ln N + C \quad N \gg 1 \quad (2.22)$$

where, $C = 0.57721 \dots$ is Euler's constant, and

$$\sum_{n=1}^N \frac{(1-\alpha)^n}{n} = -\ln \alpha \quad (2.23)$$

Substituting (2.22) and (2.23) into (2.21) yields,

$$\begin{aligned} \rho_0 &= \frac{1}{\beta} \left[\sum_{n=1}^N \frac{1}{n} - \sum_{n=1}^N \frac{(1-\alpha)^n}{n} \right] \\ &= \frac{1}{\beta} [\ln N + C - \ln \alpha] \end{aligned} \quad (2.24)$$

For $N \geq 20$, the asymptotic result is a good approximation. From (2.24) and (2.19) we obtain

$$\bar{P}_{be} = \frac{\rho_0}{\beta} = \frac{1}{\beta^2} [\ln N + C + \ln \alpha] \quad (2.25)$$

This shows the logarithmic dependence of \bar{P}_{be} on N . For MFSK, ($\alpha = \frac{1}{2}$, $\beta = \frac{1}{2}$).

$$\bar{P}_{be} = \frac{1}{\beta^2} [2 \ln N - 0.23187], \quad N \gg 1, \quad \beta \gg 1 \quad (2.26)$$

For large N and general values of ρ , a useful approximation technique can be applied here. When N is large, we can approximate the function $g(\rho)$ defined before as,

$$g(\rho) = [1 - (1 - \alpha e^{-5\rho})^N]$$

by a step function.

This implies that we can write \bar{P}_{be} as, approximated by the cumulative distribution function of ρ evaluated at some $\rho = \rho'$.

$$\bar{P}_{be} \approx \int_0^{\rho'} g(\rho) d\rho = F(\rho') \quad (2.27)$$

where ρ' is selected to be the value of ρ for which $g(\rho) = \frac{1}{2}$. A slightly more accurate approach would be to choose that value of ρ which makes equality between the integral of $g(\rho)$ and the integral of its approximation. But, the integral of $g(\rho)$ is just the general expression for \bar{P} , so that $\rho' = \rho_0$.

For Rayleigh fading, the step function approximation for \bar{P}_{be} is,

$$\bar{P}_{be} \approx F(\rho_0) = 1 - e^{-\rho_0/\bar{\rho}} \quad (2.28)$$

The use of ρ_0 in equation (2.28) leads to the required asymptotic value of \bar{P}_{be} for large $\bar{\rho}$, i.e. $\lim_{\bar{\rho} \rightarrow \infty} \bar{P}_{be} = 0$.

The values of \bar{P}_{be} for NCFSK given by the exact expression (2.17), and the asymptotic expressions for large $\bar{\rho}$ given by (2.19) and for large N given by (2.28) which uses step function approximation are compared. The results demonstrate an excellent accuracy of the step function approximation. For $N=10$ and $\bar{\rho} = 0$ dB, the error is only 5.2 percent and for $N=10$ and $\bar{\rho} = 40$ dB, the error is less than 0.02 percent.

2.3 SYSTEM PERFORMANCE

The general expression for the nonpersistent CSMA throughput is given by (2.5). For NCFSK ($\alpha = \frac{1}{2}$, $\beta = \frac{1}{2}$), substituting the general expression (2.17) for the average probability of block error \bar{P}_{be} , in equation (2.5) for the probability of packet error P_{pe} and the probability of acknowledgement error P_{ae} , we get,

$$\begin{aligned}
 S &= \frac{G e^{-aG}}{G(1+2a) + e^{-aG}} (1 - P_{pe}) (1 - P_{ae}) \quad (2.5) \\
 &= \frac{G e^{-aG}}{G(1+2a) - e^{-aG}} \cdot {}_2F_1\left(\frac{2}{\rho_p}, -N_p; 1 + \frac{2}{\rho_p}; 1/2\right) \\
 &\quad \cdot {}_2F_1\left(\frac{2}{\rho_a}, -N_a; 1 + \frac{2}{\rho_a}; 1/2\right) \quad (2.29)
 \end{aligned}$$

where ${}_2F_1(\cdot)$ is the hypergeometric function defined before and the subscript "p" refers to packet quantities and the subscript "a" refers to acknowledgement quantities.

For large block sizes, we obtained before the closed form expression for \bar{P}_{be} for NCFSK using step function approximation. Substitution of equation (2.28) into equation (2.5) leads to

$$\begin{aligned}
 S &= \frac{G e^{-aG}}{G(1+2a) - e^{-aG}} (e^{-\rho_0/\bar{\rho}_p}) (e^{-\rho_0/\bar{\rho}_a}) \\
 &= \frac{G \exp\left(-aG - \frac{\rho_0(N_p)}{\bar{\rho}_p} - \frac{\rho_0(N_a)}{\bar{\rho}_a}\right)}{G(1+2a) - e^{-aG}} \quad (2.30)
 \end{aligned}$$

where the functional dependence of the asymptotic coefficient ρ_0 on N is explicitly indicated. For NCFSK ($\alpha = \frac{1}{2}$, $\beta = \frac{1}{2}$) from equation (2.24),

$$\rho_0(N) = 2 \ln N - 0.23187 \quad (2.31)$$

For a 1000-bit packet ($N_p = 1000$), a 100-bit acknowledgement ($N_a = 100$) and equal bit-energy-to-noise density ratios (i.e. $\bar{P}_p = \bar{P}_a = \bar{P}$), we obtain,

$$S = \frac{G \exp\left(-aG - \frac{22.5621}{\bar{P}}\right)}{G(1-2a) - e^{-aG}} \quad (2.32)$$

and

$$\lim_{a \rightarrow 0} S = \frac{G \exp\left(-\frac{22.5621}{\bar{P}}\right)}{1 - G} \quad (2.33)$$

The expression (2.32) gives the nonpersistent CSMA channel throughput for NCFSK over Rayleigh fading mobile radio channel, and is plotted in Figure (2.1) for the normalized propagation delay, $a = 0.01$. The equation (2.33) shows that, when $a = 0$, a throughput of 1 can theoretically be attained for an infinite offered channel traffic and an infinite average signal-to-noise power ratio.

The general expression for the average packet delay, D , is given by equation (2.11). Substituting the closed form expressions for the probabilities of error, \bar{P}_{pe} and \bar{P}_{ae} , from equation (2.28) we obtain,

$$D = R + 1 + \left(R + \frac{K+1}{2}\right) \left[\left(\frac{G(1 - 2a) - e^{-aG}}{\exp(-aG)} \right) \left(\frac{1}{e^{-\rho_0/\rho_p} - \rho_0/\rho_p} \right)^{-1} \right]$$

$$D = R - 1 + \left(R + \frac{K-1}{2}\right) \left[\frac{G(1 + 2a) + e^{-aG}}{\exp(-aG - \frac{\rho_0}{\rho_p} - \frac{\rho_0}{\rho_e})} - 1 \right]$$

$$D = R + 1 + \left(R + \frac{K+1}{2}\right) \left[\frac{G(1 + 2a) + e^{-aG}}{\exp(-aG - \frac{22.5621}{\bar{\rho}})} - 1 \right] \quad (2.34)$$

We have plotted this packet delay expression as a function of the throughput, S, in figure (2.4). These curves provide a tradeoff for the two key system parameters, S and D.

PROBABILITY OF BLOCK ERROR IN FAST FADING

First we will start with the model suggested in [15] for rapid fading in h.f. long distance propagation. The distribution function of the amplitude strength under the fading assumption takes the form:

$$P_R(r) = \frac{2}{\Gamma(m)} \cdot \left(\frac{m}{\Omega}\right)^m R^{2m-1} \exp\left(-\frac{mR^2}{\Omega}\right) \quad R \geq 0, m \geq \frac{1}{2} \quad (2.35)$$

Where $\Omega = \overline{R^2}$

$$m = \frac{\overline{R^2}^2}{(\overline{R^2} - \overline{R^2})^2}$$

is the inverse of the normalized variance of R^2 .

Following a similar approach as in [16] one can write the signal to noise ratio SNR as:

$$\gamma = \frac{R^2}{2N}$$

where N is the output noise intensity.

Hence the p.d.f. of γ will be ,

$$P_{\gamma}(\gamma) = \frac{1}{|J|} P_R(r) \Big|_{r = \sqrt{2N\gamma}} \quad (2.36)$$

where $|J| = \frac{d\gamma}{dR}$

$$|J| = \frac{R}{N} = \frac{(2N\gamma)^{\frac{1}{2}}}{N} = \left(\frac{2\gamma}{N}\right)^{\frac{1}{2}}$$

$$\begin{aligned} \text{Then, } P_{\gamma}(\gamma) &= \left(\frac{2\gamma}{N}\right)^{-\frac{1}{2}} \frac{2}{\Gamma(m)} \left(\frac{m}{\Omega}\right)^m (2N\gamma)^{\frac{1}{2}(2m-1)} \exp\left[-\frac{m}{\Omega} 2N\gamma\right] \\ &= \frac{(2N)^m}{\Gamma(m)} \left(\frac{m}{\Omega}\right)^m \gamma^{m-1} \exp\left(-\frac{m}{\Omega} 2N\gamma\right) \\ &= \left(\frac{2Nm}{\Omega}\right)^m \frac{1}{\Gamma(m)} \gamma^{m-1} \exp\left(-\frac{m}{\Omega} 2N\gamma\right) \end{aligned} \quad (2.37)$$

which can be recognized as a Gamma distribution with parameters $K = \frac{2Nm}{\Omega}$, m , where both of them can only take positive values.

For a packet length of N bits and a NCFSK modulation scheme, the probability that at least one bit in the block is in error takes the form [16]

$$P_{be} = 1 - \left(1 - \frac{1}{2} e^{-\frac{\gamma}{2}}\right)^N \quad (2.38)$$

Averaging equation (2.38) over the fading signal level will be

$$\bar{P}_{be} = \int_0^{\infty} \left[1 - \left(1 - \frac{1}{2} e^{-\frac{\gamma}{2}}\right)^N\right] \frac{k^m}{\Gamma(m)} \gamma^{m-1} e^{-k\gamma} d\gamma \quad (2.39)$$

where $k = \frac{2Nm}{\Omega}$

$$\text{Then } \bar{P}_{be} = 1 - \frac{k^m}{\Gamma(m)} \int_0^{\infty} \left(1 - \frac{e^{-\frac{\gamma}{2}}}{2}\right)^N e^{-k\gamma} \gamma^{m-1} d\gamma$$

$$\text{But } \left(1 - ke^{-kx}\right)^N = \sum_{q=0}^N \binom{N}{q} e^{-qkx} (k)^q \quad (2.40)$$

$$\text{Then } \bar{p}_{be} = 1 - \frac{k^m}{\Gamma(m)} \sum_{q=0}^N \binom{N}{q} \left(\frac{1}{2}\right)^q \int_0^{\infty} e^{-\frac{\gamma}{2} - k\gamma} \gamma^{m-1} d\gamma \quad (2.41)$$

After a substitution of $\gamma(k + \frac{q}{2}) = \theta$

we obtain,

$$\begin{aligned} \bar{p}_{be} &= 1 - \frac{k^m}{\Gamma(m)} \sum_{q=0}^N \binom{N}{q} \left(\frac{1}{2}\right)^q \int_0^{\infty} \frac{e^{-\theta} \theta^{m-1}}{(k+q)^m} d\theta \\ &= 1 - \frac{k^m}{\Gamma(m)} \sum_{q=0}^N \binom{N}{q} \left(\frac{1}{2}\right)^q \left(\frac{1}{k+q}\right)^m \Gamma(m) \end{aligned} \quad (2.42)$$

or

$$\bar{p}_{be} = 1 - k^m \sum_{q=0}^N \binom{N}{q} \left(\frac{1}{2}\right)^q \frac{1}{(k+q)^m} \quad (2.43)$$

We can easily evaluate equation (2.43) when the constants N, K, m are specified.

Substituting equation (2.43) for \bar{p}_{be} one can obtain the modified expressions for both the channel throughput and the average packet delay when rapid fading is considered.

2.5 SUMMARY AND DISCUSSION

Nonpersistent CSMA mobile packet radio performance in slow Rayleigh fading has been characterized in terms of throughput and average packet delay versus bit energy-to-noise density ratio and size of the packet and acknowledgement bit.

The throughput, (5) versus offered channel traffic (G) plot, in Figure (2.1) shows strong dependence of throughput on the average signal-to-noise power ratio, $\bar{\rho}$.

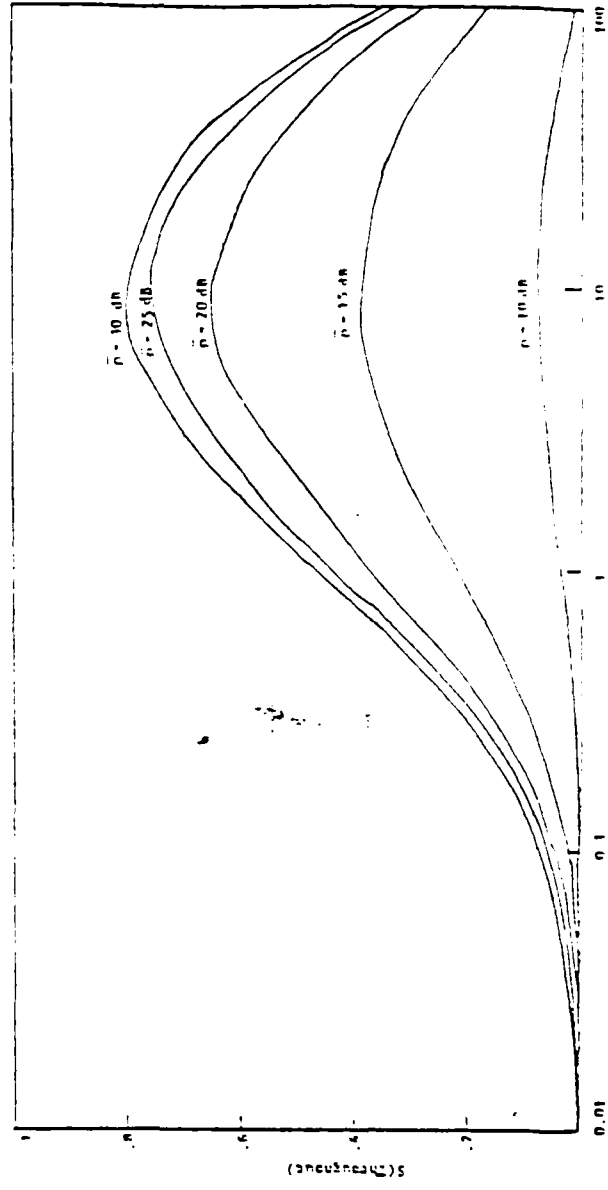
The average number of times a packet was scheduled for transmission before success given by G/S is plotted versus throughput S in Figure (2.2). Lower values of G/S are obtained for higher SNR and for average SNR of about 30 dB the performance is close to the conventional nonpersistent CSMA case. The 'channel capacity', defined as the maximum achievable throughput, is plotted in Figure (2.3) as a function of the propagation delay (a). We note that the channel capacities are sensitive to increase in a . For large a , the performance drops considerably.

The average packet delay versus throughput curves presented in Figure (2.4) indicate higher delay for low average SNR. Also, these curves show that it is possible to design a packet radio system for nonfading environment such that when fading is encountered, the only effect on system performance is an increase in average packet delay.

The analysis in this chapter was based on the assumption that all terminals are within range and in line-of-sight of each other.

Each terminal, however, may not be able to hear all the other terminal's traffic. This gives rise to the "hidden terminals" problem, which badly degrades the performance of CSMA.

The analytical results obtained in this chapter can be extended to study the performance of ETMA mobile packet radio channels.



C (offered channel Traffic)

Figure 2.1. Dependence of channel throughput on offered channel traffic for $\lambda = 1000$ bits/sec, $\mu = 1000$ bits/sec, $\sigma = 100$ bits/sec

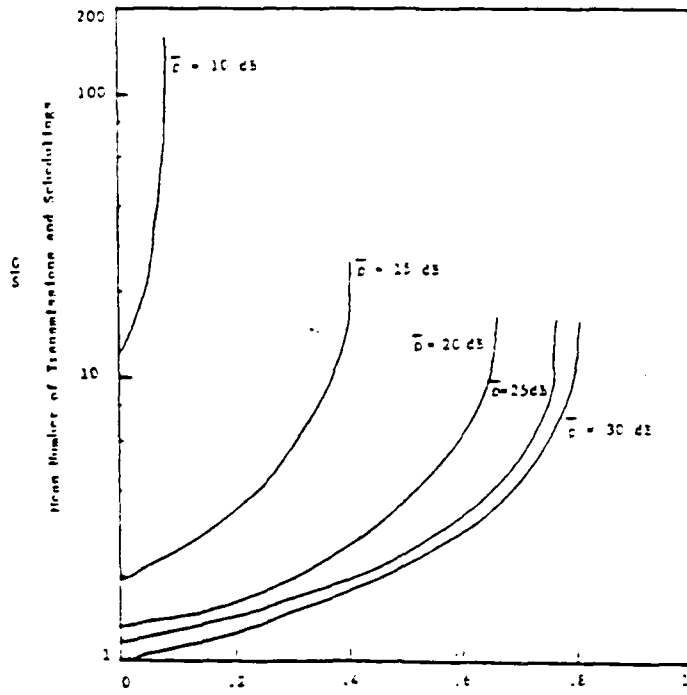


Figure 2.1 Mean Number of Transmissions and Retransmissions versus channel throughput S in fading channel.
 ($\lambda = 0.01$) MCTS = 1000 bit packet, 100 bit ack.

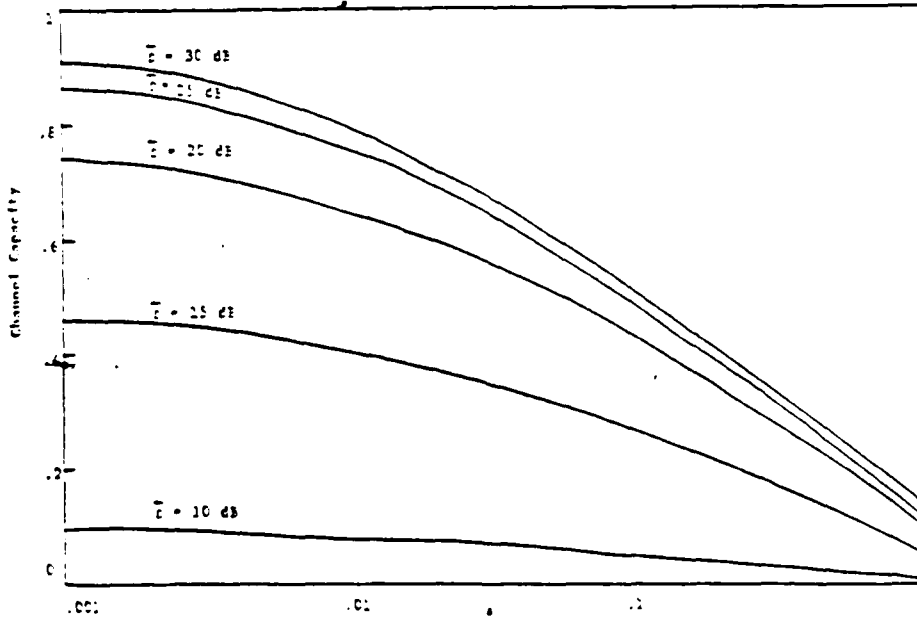


Figure 2.2 Effect of propagation delay on channel capacity in fading channel. MCTS = 1000-bit packet, 100-bit acknowledgement.

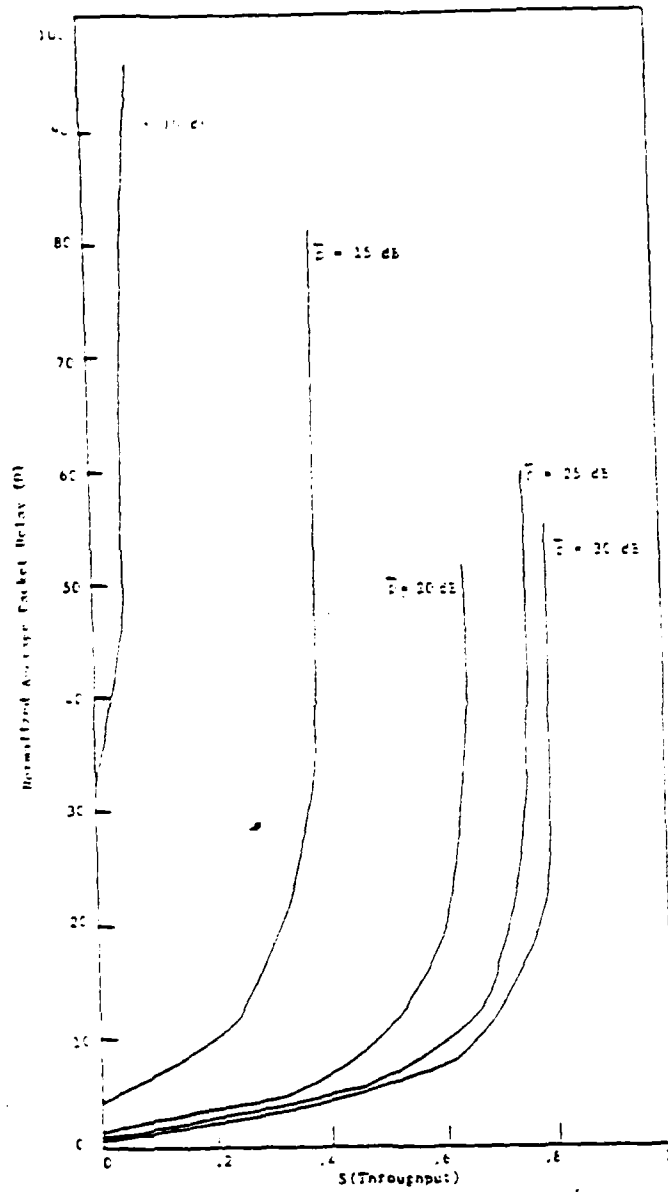


Figure 2.4 Average Packet Delay versus channel throughput, S is fading channel. ($\alpha = 0.01$) - QPSK - 1000 bit packet - 100 bit/sec.

CHAPTER III

PERFORMANCE DEGRADATION DUE TO HIDDEN TERMINAL PROBLEM IN CARRIER SENSE MULTIPLE ACCESS FOR MOBILE PACKET RADIO CHANNELS

We consider a population of terminals communicating with a central station over a packet-switched multiple-access mobile radio channel. The performance of CSMA used as a method for multiplexing these terminals is highly dependent on the ability of each terminal to sense the carrier of any other transmission on the channel. Many situations exist in which some terminals are "hidden" from each other (either because they are out-of-sight or out-of-range). In this chapter, we show that the existence of hidden terminals significantly degrades the performance of CSMA in mobile packet radio channels. The channel throughput expressions are derived for the nonpersistent CSMA single-hop mobile packet radio system operating in slow Rayleigh fading with and without hidden terminals. The dynamic block error rate for slow nonselective Rayleigh fading is derived for the coherent data transmission techniques, viz, CPSK, MSK, GMSK, and CFSK, using an excellent approximation technique for large packet sizes. Numerical results giving the channel capacity and the offered channel traffic rate are tabulated

and the behavior of system parameters for Gaussian Minimum Shift Keying are shown as it is considered a potential digital modulation technique for future mobile radio telephone services.

3.1 NON-PERSISTENT CSMA WITH HIDDEN TERMINALS

The model described in [17] is used to study the hidden terminal problem in CSMA. We assume an environment consisting of a large number of terminals communicating with a single station over a shared mobile radio channel characterized by Rayleigh fading and AWGN. All terminals are in line-of-sight and within range of the station but not necessarily with respect to each other. The total traffic source is approximated by an independent Poisson source with an aggregate mean packet generation rate of λ packets/sec.

A terminal configuration with hidden elements is characterized as follows: Let $i = 1, 2, \dots, M$ index the M terminals in the population. By definition, terminal i "hears" (is connected to) terminal j if i and j are within range and in line-of-sight of each other. In order to represent terminal configurations with hidden elements, it is advantageous to partition the population into several groups (say, N , $N \leq M$) such that all terminals in a group hear exactly the same subset of terminals in the population. It is further assumed that each group i consists of a large number of users who collectively form an independent Poisson source with an aggregate mean packet generation rate

λ_i packet/s such that

$$\sum_{i=1}^N \lambda_i = \lambda \quad (3.1)$$

For nonpersistent CSMA, the probability of success [17] of an arbitrary packet from group i is given as,

$$P_{S_i} = \frac{S_i}{G_i} = \exp [G_i(1-2a)] \prod_{j=1}^N \frac{\exp[-G_j(1-a)]}{G_j(1-2a) - \exp[-2G_j]} \quad (3.2)$$

consider the particular case of N independent and identical groups, i.e.,

$$S_i = s \quad \forall_i$$

$$G_i = g \quad \forall_i$$

The probability of success reduces to,

$$P_S = \frac{S}{G} = \frac{s}{g} = \exp [g(1-2a)] \left[\frac{\exp[-g(1-a)]}{g(1-2a) - \exp[-2g]} \right]^N \quad (3.3)$$

If we let $N \rightarrow \infty$, $s \rightarrow 0$, and $g \rightarrow 0$ such that $Ns = S$ and $Ng = G$, the CSMA mode reduces to the ALOHA access mode, i.e.

$$\frac{S}{G} \xrightarrow{N \rightarrow \infty} e^{-2G}$$

the probability of success of a packet in ALOHA mode.

If the packet channel is fading and the acknowledgement channel is not error-free due to fading then the modified expression for the probability of success of the packet results [18];

$$P_S = \frac{S}{G} = \exp [g(1-2a)] \left[\frac{\exp[-g(1-a)]}{g(1-2a) - \exp[-2g]} \right]^N (1 - P_{pe})(1 - P_{ae}) \quad \dots (3.4)$$

Therefore, the channel throughput for the nonpersistent CSMA for hidden terminal configuration is given by,

$$S = G \exp[g(1 - 2a)] \left[\frac{\exp[-g(1 - a)]}{g(1 + 2a) + \exp(-2g)} \right]^N (1 - P_{pe})(1 - P_{ae}) \quad \dots(3.5)$$

where the parameter a is the ratio of propagation delay (τ) to packet transmission time (T), and is called normalized delay.

3.2 DYNAMIC BLOCK ERROR RATE

Consider a block of length N bits corresponding to either a packet or an acknowledgement. The probability of block error P_{be} , is the probability of at least one bit error in the block and is given by,

$$P_{be} = 1 - [1 - e(p)]^N \quad (3.6)$$

When a quasi-stationary slow Rayleigh fading model is assumed, dynamic block error rate performance is given by the probability of block error averaged over the fading signal level,

$$\begin{aligned} \bar{P}_{be} &= \int_0^{\infty} P_{be} f(\rho) d\rho \\ &= \int_0^{\infty} [1 - [1 - \epsilon(\rho)]^N] \epsilon(\rho) d\rho \end{aligned} \quad (3.7)$$

where, ρ is assumed constant over the block length and $f(\rho)$ is the probability density function (pdf) of ρ given by,

$$f(\rho) = \frac{1}{\bar{\rho}} \exp\left(-\frac{\rho}{\bar{\rho}}\right), \quad \rho \geq 0 \quad (3.8)$$

where $\bar{\rho}$ is the average value of ρ .

For the coherent signaling subject to AWGN, the bit error probability function is given by [11],

$$\epsilon(\rho) = \frac{1}{2} \operatorname{erfc}(\sqrt{C\rho}) \quad (3.9)$$

where $\operatorname{erfc}(\cdot)$ is the complementary error function given by,

$$\operatorname{erfc}(x) \triangleq \frac{2}{\sqrt{\pi}} \int_x^{\infty} \exp(-u^2) du \quad (3.10)$$

and C is a constant parameter defined for particular modulation scheme as follows [11, 19];

$$\left. \begin{aligned} C &= 1.0, \text{ for CPSK} \\ &= 0.50, \text{ for orthogonal CPSK} \\ &= 0.85, \text{ for simple MSK } (E_b/T = \infty) \\ &= 0.68, \text{ for GMSK } (E_b/T = 0.25) \end{aligned} \right\} \quad (3.11)$$

where, T is bit period and B_b is the variable bandwidth of the premodulation Gaussian LPF [19]. For example, when bit rate $f_b = 16$ Kbps, the bandwidth B_b is chosen as 4 KHz to achieve $B_b T$ of 0.25 for GMSK.

Substitution of equations (3.8) and (3.9) into (3.7) yields an integral given by,

$$\bar{P}_{be} = \frac{1}{P} \int_0^{\infty} \left[1 - \left[1 - \frac{1}{2} \operatorname{erfc}(\sqrt{cP}) \right]^N \right] \exp\left(-\frac{P}{c}\right) dP \quad (3.12)$$

This integral cannot be evaluated in closed form. Hence, we are tempted to rely on some approximation technique to evaluate \bar{P}_{be} . There exists an excellent approximation technique for large packet sizes, which is used in [18] to derive closed form expression for \bar{P}_{be} for noncoherent modulation schemes.

For large N and general values of \bar{P} , we can approximate

$$g(P) = 1 - [1 - e(P)]^N \quad (3.13)$$

by a step function. This leads to

$$\bar{P}_{be} = \int_0^{P'} f(P) dP = F(P') \quad (3.14)$$

i.e. probability of block error averaged over the fading signal level (\bar{P}_{be}) is approximated by the cumulative

distribution function (CDF) of ρ evaluated at some point $\rho = \rho'$ where ρ' is chosen as $\rho' = \rho_0$.

For Rayleigh fading, the step function approximation for \bar{P}_{be} is,

$$\bar{P}_{be} = F(\rho_0) = 1 - e^{-\rho_0/\bar{\rho}} \quad (3.15)$$

where

$$\begin{aligned} \rho_0 &\triangleq \int_0^{\infty} g(\rho) \, d\rho \\ &= \int_0^{\infty} [1 - [1 - E(\rho)]^N] \, d\rho \\ &= \int_0^{\infty} [1 - [1 - \frac{1}{2} \operatorname{erfc}(\sqrt{c\rho})]^N] \, d\rho \\ &= \frac{1}{c} \int_0^{\infty} [1 - [1 - \frac{1}{2} \operatorname{erfc}(\sqrt{x})]^N] \, dx \end{aligned} \quad (3.16)$$

This expression is computed numerically for different coherent modulation schemes under study.

3.3 SYSTEM PERFORMANCE

The average probability of block error for the channel degraded with slow Rayleigh fading is derived for coherent modulation schemes under consideration. The analysis for channel throughput is presented for the nonpersistent CSMA

without and with hidden terminals in fading environment for coherent data transmission techniques.

NONPERSISTENT CSMA with no hidden terminal: The channel throughput given by (3.1) takes the following form after substituting for the probabilities P_{pe} and P_{ae} from equation (3.15),

$$S = \frac{Ge^{-aG}}{G(1-2a) - e^{-aG}} \left(e^{-\rho_0/\bar{\rho}_p} \right) \left(e^{-\rho_0/\bar{\rho}_a} \right)$$

$$= \frac{G \exp \left\{ -aG - \frac{\rho_c(N_p)}{\bar{\rho}_p} - \frac{\rho_c(N_a)}{\bar{\rho}_a} \right\}}{G(1-2a) - e^{-aG}} \quad (3.17)$$

where functional dependence of the coefficient ρ_0 on the block size N is explicitly indicated. The throughput expression (3.17) holds good for large block sizes and has been developed using step function approximation.

For a 1000-bit packet ($N_p = 1000$), a 100-bit acknowledgement ($N_a = 100$), and equal bit-energy-to-noise density ratios (i.e. $\bar{\rho}_p = \bar{\rho}_a = \bar{\rho}$), numerical computation of equation (3.16) yields

$$\left. \begin{aligned} \rho_0(N_p) &= \frac{1}{2} (5.315) \\ \rho_0(N_a) &= \frac{1}{2} (3.236) \end{aligned} \right\} \quad (3.18)$$

This implies that, throughput expression (3.16) becomes,

$$S = \frac{G \exp\left(-aG - \frac{8.551}{c\bar{P}}\right)}{G(1 - 2a) - e^{-aG}} \quad (3.19)$$

where parameter c is defined by (3.11) for the modulation scheme considered.

The channel throughputs are evaluated from equation (3.19) for the various modulation schemes, for the normalized propagation delay, $a=0.01$. The "channel capacity" defined as the maximum throughput is tabulated in Table 6.1 for different values of the average SNR. The throughput equations show that when delay $a = 0$ and average SNR is infinite, theoretically, throughput of unity can be achieved for an infinite offered channel traffic (G).

NONPERSISTENT CSMA with hidden terminals: The channel throughput given by (3.5) takes the following form after substituting for the probabilities P_{pe} and P_{ae} from (3.15),

$$\begin{aligned}
S &= G \exp[g(1 - 2a)] \left[\frac{\exp[-g(1-a)]}{g(1+2a) + \exp(-ag)} \right]^N (e^{-\rho_0/\bar{\rho}_p}) (e^{-\rho_0/\bar{\rho}_e}) \\
&= G \exp[g(1 - 2a)] \left[\frac{\exp[-g(1-a)]}{g(1+2a) + \exp(-ag)} \right]^N \exp\left(-\frac{\rho_0(N_p)}{\bar{\rho}_p} - \frac{\rho_0(N_e)}{\bar{\rho}_e}\right) \\
&\dots (3.20)
\end{aligned}$$

Invoking equation (3.18) here again, we obtain for channel throughput,

$$S = G \exp[g(1 - 2a)] \left[\frac{\exp[-g(1-a)]}{g(1+2a) + \exp(-ag)} \right]^N \exp\left(-\frac{8.551}{a\bar{\rho}}\right) \quad (3.21)$$

The channel throughputs are evaluated from equation (3.21) for the various modulation schemes for $a = 0.01$. The channel capacity is tabulated in Table 3.2 for different group size N and for the average SNR varying from 10 dB to 50 dB, under a symmetric configuration assumption.

3.4 SUMMARY AND DISCUSSION

The performance of nonpersistent CSMA mobile packet radio channel has been analyzed in slow Rayleigh fading. The step function approximation yields closed form expressions for the channel throughput for large packet sizes. The numerical results for the various coherent data transmission techniques have been tabulated in Table 3.1 for the case of no hidden terminals and in Table 3.2 for the case of hidden

terminals. The results are illustrated in detail for GMSK technique due to its suggested importance in mobile radio telephone services.

The complexity of the equipment and the implementation of the protocol is directly related to the number of schedulings and transmissions that a packet incurs. The average number of schedulings and transmissions (G/S) has been plotted against the channel throughput (S) in figure (3.2)

Table 3.2 shows the channel capacity (C) available and the corresponding offered channel traffic rate (G) for the various modulation schemes and for the number of independent groups (N) varying from 1 to 10. We have considered the case in which the population is partitioned into N independent

Table 8.1 shows that channel capacity for the CPSK technique is the highest amongst all the coherent techniques under consideration. At average SNR of 10 dB, the channel capacity is below that of slotted ALOHA but at about 15 dB, nonpersistent CSMA performs better than slotted ALOHA. In figure (3.2), the channel throughput (S) has been plotted against the offered traffic rate (G) for SNR varying from 10 - 30 dB.

Table 3.2 shows the channel capacity (C) available and the corresponding offered channel traffic rate (G) for the various modulation schemes and for the number of independent groups (N) varying from 1 to 10. We have considered the case in which the population is partitioned into N independent

groups of equal size and a symmetric configuration is studied. For each terminal there exists [17] a fraction of the population which is hidden, namely $\beta = \frac{N-1}{N}$ (> 0.5). For $N=1$ ($\beta = 0$) there is no hidden terminal and the performance is same as obtained in Table 3.1. From the Table 3.2, it is noticed that for $\bar{p} < 15$ dB, CFSK performs poorer than pure ALOHA, whereas others are close to pure ALOHA. The performance of nonpersistent CSMA with hidden terminals is almost independent of the modulation scheme for $\bar{p} \geq 35$ dB.

The channel capacity for various values of N is plotted in figure (3.3) for GMSK mode. Notice that the channel capacity experiences a drastic decrease between the two cases: $N=1$; (no hidden terminals, $\beta=0$) and $N=2$ ($\beta=0.5$). For $N > 2$, the channel capacity is rather insensitive to N and approaches pure ALOHA, for large N if $\bar{p} > 20$ dB, otherwise it is lower than pure ALOHA. For $N \geq 2$, the performance is poorer than slotted ALOHA. In figure (3.4), we have plotted channel throughput versus offered channel traffic rate for GMSK technique, and in figure (3.5) average number of schedulings and retransmissions versus channel throughput. Note that delay (proportional to G/S) reduces for higher average SNR and also throughput improves but is still lower than slotted ALOHA.

The performance degradation due to hidden terminals in nonpersistent CSMA protocol for mobile packet radiochannels is illustrated. To eliminate this problem in single-station environments, the use of busy-tone channel [20] may be considered.

Table 3.1 Nonpersistent CSMA with no hidden terminals ($\alpha = 0.01$) for multi-packet radio channels

Average SNR $\bar{p}(dB)$	Offered Channel Traffic (ρ) and Channel Capacity (C)							
	Data Transmission Techniques							
	CFR		CRS		MS		CFR	
	ρ	C	ρ	C	ρ	C	ρ	C
10	7.50	.147	8.50	.020	8.50	.298	9.00	.547
15	8.50	.275	9.50	.348	9.00	.593	9.00	.620
20	9.00	.487	9.00	.719	9.00	.737	8.50	.748
25	9.00	.770	9.00	.783	9.00	.790	8.50	.790
30	9.00	.801	9.00	.805	9.00	.807	9.00	.806
35	9.50	.813	9.00	.810	9.00	.810	9.00	.813
40	9.50	.814	9.00	.814	9.00	.814	8.50	.814
45	9.50	.815	9.00	.815	9.00	.815	9.00	.815
50	9.00	.815	9.00	.815	9.00	.815	9.00	.815

Table 3.2 Nonpersistent CSMA with Hidden Terminals for mobile packet radio
Channels ($\alpha = 0.01$)

Average SNR $\bar{\rho}$ (dB)	Number of Independent Groups (N)	Offered Channel Traffic (R) and Channel Capacity (C)							
		Data Transmission Techniques							
		CFSA		CMSA		MSA		CPSA	
		C	E	C	E	C	E	C	E
10	1	7.50	.147	6.50	.237	6.50	.298	6.00	.347
	2	.70	.049	.70	.077	.82	.100	.76	.116
	3	.56	.042	.56	.066	.58	.083	.60	.099
	4	.50	.039	.54	.062	.56	.080	.58	.082
	5	.50	.038	.54	.060	.54	.077	.52	.089
	6	.48	.037	.48	.058	.52	.075	.50	.087
	7	.56	.037	.48	.057	.52	.074	.52	.086
	8	.46	.036	.52	.057	.50	.073	.52	.083
	9	.50	.036	.48	.056	.48	.072	.50	.084
	10	.44	.035	.50	.056	.50	.072	.48	.083
15	1	6.50	.473	6.50	.548	6.00	.593	6.00	.622
	2	.74	.258	.78	.383	.78	.398	.80	.399
	3	.64	.236	.64	.257	.64	.270	.62	.273
	4	.56	.227	.60	.247	.58	.259	.60	.267
	5	.52	.222	.54	.242	.56	.253	.54	.261
	6	.56	.220	.54	.238	.52	.249	.56	.257
	7	.54	.218	.54	.236	.52	.247	.52	.254
	8	.50	.216	.52	.234	.52	.245	.50	.252
	9	.50	.215	.52	.233	.52	.244	.52	.251
	10	.50	.214	.52	.232	.52	.243	.52	.250
20	1	6.00	.687	6.00	.729	6.00	.737	6.50	.748
	2	.76	.229	.78	.240	.78	.246	.78	.250
	3	.66	.207	.64	.206	.64	.212	.62	.214
	4	.58	.184	.62	.193	.58	.197	.56	.202
	5	.54	.177	.54	.183	.54	.190	.56	.193
	6	.54	.173	.54	.182	.56	.186	.58	.189
	7	.52	.170	.52	.178	.54	.183	.52	.185
	8	.52	.168	.52	.176	.50	.180	.52	.183
	9	.54	.167	.50	.174	.52	.179	.50	.182
	10	.50	.165	.52	.173	.50	.177	.50	.180

continued

25	1	5.00	.772	5.00	.783	5.50	.790	5.50	.793
	2	.80	.258	.82	.262	.84	.264	.84	.264
	3	.64	.221	.62	.224	.64	.226	.64	.227
	4	.60	.207	.60	.210	.62	.212	.62	.213
	5	.54	.199	.56	.202	.58	.204	.58	.205
	6	.58	.195	.52	.197	.54	.199	.54	.200
	7	.52	.191	.52	.194	.54	.196	.54	.197
	8	.52	.186	.54	.192	.52	.193	.52	.194
	9	.50	.187	.52	.190	.50	.191	.50	.192
	10	.52	.188	.50	.188	.52	.190	.52	.191
30	1	5.00	.801	5.00	.803	5.00	.807	5.00	.808
	2	.82	.268	.80	.269	.76	.269	.80	.270
	3	.62	.229	.62	.230	.64	.231	.62	.231
	4	.60	.215	.60	.216	.58	.216	.56	.216
	5	.56	.207	.58	.208	.56	.208	.58	.209
	6	.54	.202	.56	.203	.54	.203	.56	.204
	7	.56	.199	.52	.199	.54	.200	.56	.200
	8	.52	.196	.52	.197	.50	.197	.54	.198
	9	.50	.194	.52	.195	.54	.196	.52	.196
	10	.52	.195	.52	.194	.50	.194	.50	.194
35	1	5.50	.811	5.00	.812	5.00	.812	5.00	.811
	2	.80	.271	.78	.271	.76	.271	.76	.271
	3	.64	.232	.62	.232	.66	.233	.66	.233
	4	.58	.217	.56	.217	.60	.218	.60	.218
	5	.56	.209	.54	.209	.58	.210	.56	.210
	6	.54	.204	.56	.203	.56	.203	.56	.203
	7	.56	.201	.52	.201	.52	.201	.52	.201
	8	.50	.198	.54	.199	.52	.199	.52	.199
	9	.54	.197	.52	.197	.52	.197	.52	.197
	10	.50	.195	.50	.195	.54	.196	.54	.196
40	1	5.50	.814	5.00	.814	5.00	.814	5.50	.814
	2	.80	.272	.80	.272	.78	.272	.78	.272
	3	.64	.233	.64	.233	.64	.233	.64	.233
	4	.58	.218	.58	.218	.58	.218	.58	.218
	5	.56	.210	.56	.210	.56	.210	.56	.210
	6	.54	.205	.54	.203	.54	.203	.54	.203
	7	.56	.202	.54	.202	.54	.202	.54	.202

continued

	E	.52	.194	.52	.194	.52	.194	.52	.194
	4	.50	.197	.50	.197	.50	.197	.50	.197
	10	.52	.196	.52	.196	.52	.196	.52	.196
45	1	5.50	.815	5.00	.815	5.00	.815	5.00	.815
	2	.78	.272	.78	.272	.78	.272	.78	.272
	3	.62	.233	.62	.233	.62	.233	.62	.233
	4	.58	.218	.58	.218	.58	.218	.58	.218
	5	.56	.210	.54	.210	.54	.210	.54	.210
	6	.54	.205	.54	.205	.54	.205	.54	.205
	7	.54	.202	.54	.202	.54	.202	.54	.202
	8	.52	.199	.50	.199	.50	.199	.50	.199
	9	.50	.197	.54	.198	.54	.198	.54	.198
	10	.52	.196	.50	.196	.50	.196	.50	.196
50	1	5.00	.815	5.00	.815	5.00	.815	5.00	.815
	2	.78	.272	.78	.272	.78	.272	.78	.272
	3	.62	.233	.62	.233	.62	.233	.62	.233
	4	.58	.218	.58	.218	.58	.218	.58	.218
	5	.54	.210	.54	.210	.54	.210	.54	.210
	6	.54	.205	.54	.205	.54	.205	.54	.205
	7	.54	.202	.54	.202	.54	.202	.54	.202
	8	.50	.199	.50	.199	.50	.199	.50	.199
	9	.54	.198	.54	.198	.54	.198	.54	.198
	10	.50	.196	.50	.196	.50	.196	.50	.196

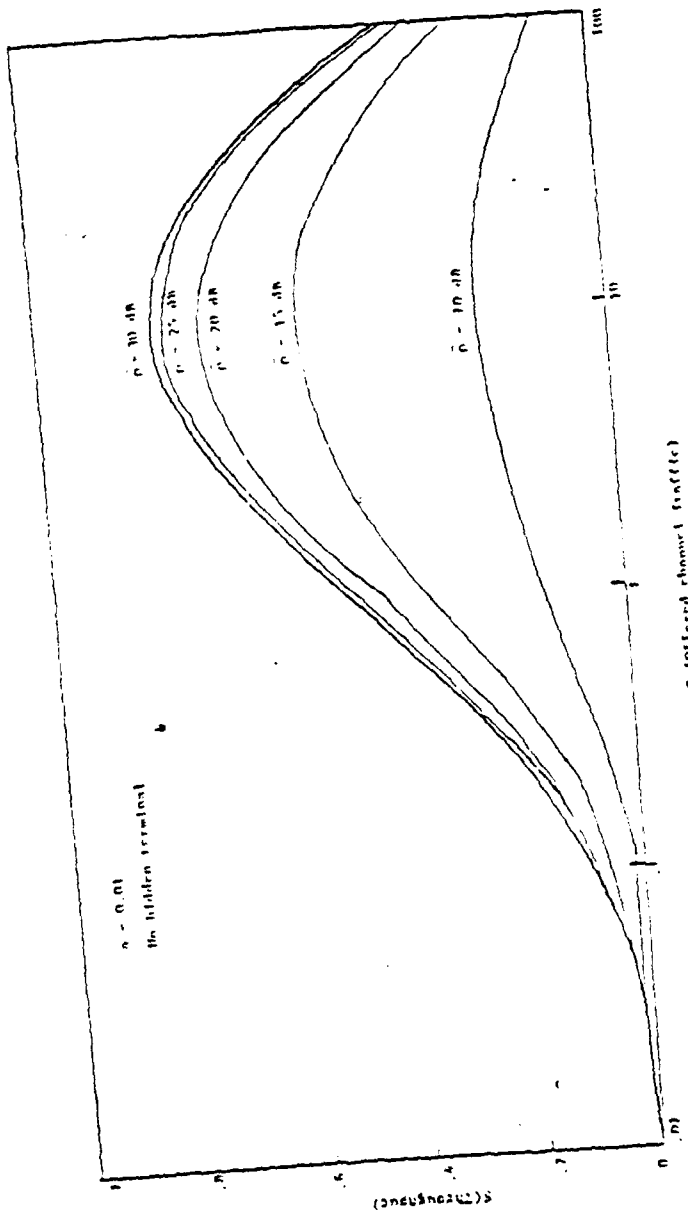


Figure 3.1 Noncoherent CDMA channel throughput in fading channel for CDMA - 1000-bit packet - 100-bit msg.

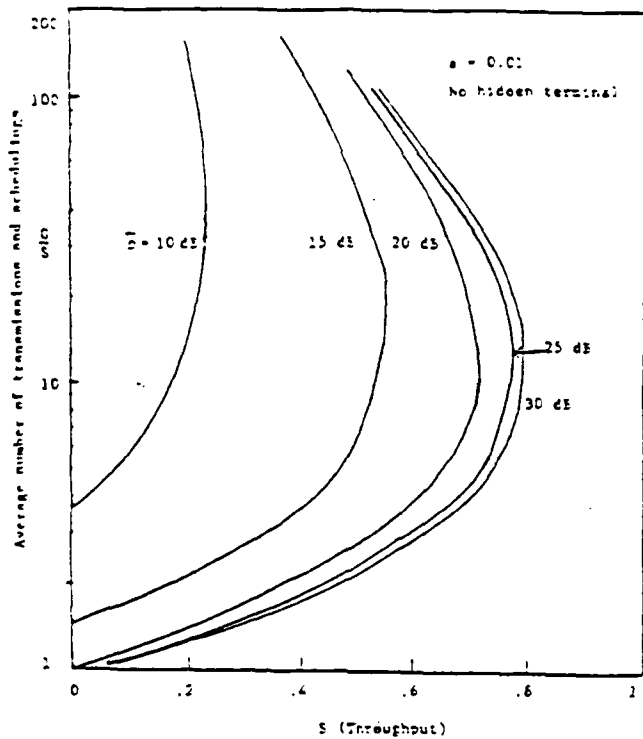


Figure 3.2 G/S versus channel throughput S to facing channel for QPSK = 1000-bit packet, 100-bit ACK.

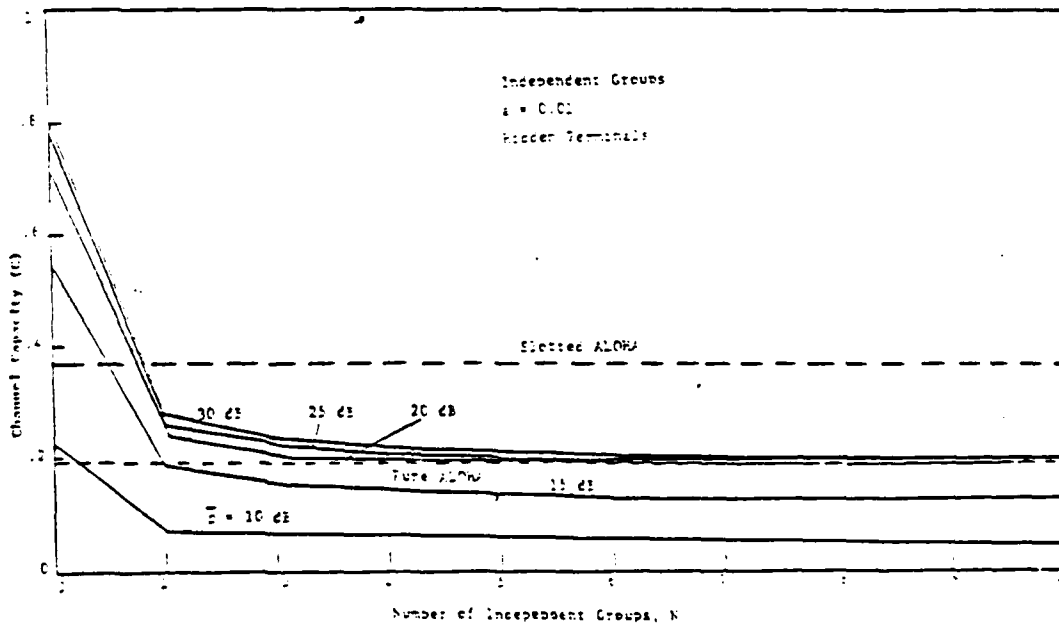


Figure 3.3 Channel capacity versus the number of independent groups for nonpersistent CSMA receive their channel with QPSK modulation.

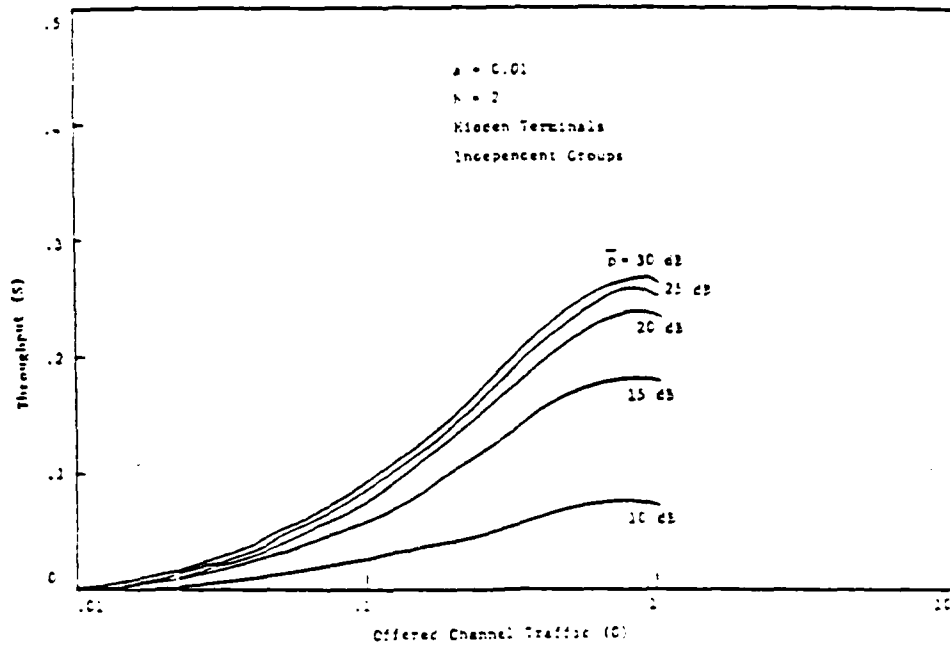


Figure 3.4 Channel Throughput versus offered channel traffic for nonpersistent CSMA mobile radio channel with GMSK modulation.

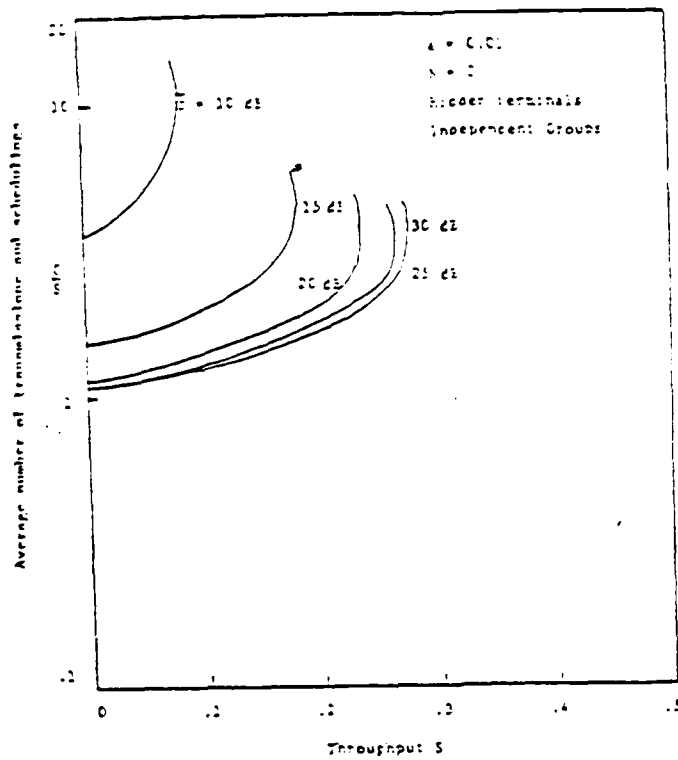


Figure 3.5 C/S versus channel throughput S for nonpersistent CSMA mobile radio channel with GMSK modulation.

CHAPTER IV

CARRIER SENSE MULTIPLE ACCESS WITH COLLISION DETECTION FOR FH/FSK SPREAD SPECTRUM MOBILE PACKET RADIO NETWORKS

The performance of nonpersistent CSMA-CD protocol for the FH/FSK Spread Spectrum mobile packet radio network (MPRNET) is studied in this chapter. The mobile radio network link is modeled as consisting of separate and independent message channel and acknowledgement channel. Both are considered as Rayleigh fading AWGN Channels. Probability of block error for slow Rayleigh fading is derived for FH/FSK scheme in the presence of partial-band noise interference. The modified expression for the channel throughput is derived for the CSMA-CD protocol in the context of ground mobile radio channel employing FH/FSK Spread Spectrum Communication. The throughput performance of CSMA-CD and its dependence on such key system parameters as the offered channel traffic, Collision recovery time, channel capacity, packet transmission time, and signal-to-noise power ratio are provided.

4.1 INTRODUCTION

We have chosen a spread spectrum (SS) scheme [1] to analyze the performance of the CSMA/CD MPRNET. Network aspects of spread spectrum make spread spectrum transmission an attractive candidate for packet radio network environment.

Earlier analysis of CSMA-CD [22] assumed perfect packet transmitting and acknowledgement channels, whereas in a mobile packet radio environment the effect of link errors due to noise and fading plays an important role in the performance analysis. Therefore, we need to modify the throughput-delay analysis for a fading and noisy channel. We derive the nonpersistent CSMA-CD channel throughput as a function of the probability of a packet error and an acknowledgement error assuming that the packet and acknowledgement channels are separate and independent.

The channel throughput [22] for the nonpersistent CSMA-CD scheme is given by,

$$S = \frac{\tau p e^{-\tau}}{\tau p e^{-\tau} + (1 - e^{-\tau} - \tau e^{-\tau})\gamma + 1} \quad (4.1)$$

To derive the modified throughput expression we consider the probability of success on the first packet transmission,

$$P_s = \frac{S}{G} = \frac{\tau a e^{-\tau a G}}{\tau a G e^{-\tau a G} + (1 - e^{-\tau a G} - \tau a G e^{-\tau a G})\gamma + 1} \quad (4.2)$$

where, a is the normalized propagation delay and G is the offered channel traffic.

When the ACK channel is error-free but the packet channel is fading, then probability of success on the first packet transmission is given by,

$$P_s = \left(\frac{\tau a e^{-\tau a G}}{\tau a G e^{-\tau a G} + (1 - e^{-\tau a G} - \tau a G e^{-\tau a G})\gamma - 1} \right) (1 - P_{pe}) \quad (4.3)$$

where P_{pe} is the probability of packet error. It is assumed that all packet collisions result in lost packets, however, in a collision between a faded and a nonfaded packet, the nonfaded packet might not be lost hence equation (4.3) gives a lower bound on P_s . Furthermore, if the ACK channel is also fading then acknowledgements can arrive at the user receiver in error. Let P_{ae} be the probability of ACK error then the probability of success given by equation (4.3) modifies to,

$$P_s = \left(\frac{\Gamma_a \Gamma_e^{-2G}}{\Gamma_a \Gamma_e^{-2G} + (1 - e^{-\Gamma_a \Gamma_e^{-2G}} - \Gamma_a \Gamma_e^{-2G}) \gamma + 1} \right) (1 - P_{pe})(1 - P_{ae}) \quad (4.4)$$

Therefore the desired throughput expression for the MFRNET with fading link is given by,

$$S = \left(\frac{\Gamma_a \Gamma_e^{-2G}}{\Gamma_a \Gamma_e^{-2G} + (1 - e^{-\Gamma_a \Gamma_e^{-2G}} - \Gamma_a \Gamma_e^{-2G}) \gamma + 1} \right) (1 - P_{pe})(1 - P_{ae}) \quad (4.5)$$

4.2 DYNAMIC BLOCK ERROR PROBABILITY

The probabilities of packet error (P_{pe}) and acknowledgement error (P_{ae}) appearing in the channel throughput expression (4.5) are given by the probability that a block of some number of bits is in error. We need to derive the expected value of the probability of block error for the fading channel.

Consider a block of length N bits corresponding to either a packet or an acknowledgement. The probability of block error P_{be} is given as,

$$P_{be} = 1 - (1 - \epsilon(\rho))^N \quad (4.6)$$

For a slow Rayleigh fading model, the dynamic block error probability is given by P_{be} averaged over the fading signal level,

$$\begin{aligned} \bar{P}_{be} &= \int_0^{\infty} P_{be} f(\rho) d\rho \\ &= \int_0^{\infty} [1 - (1 - E(\rho))^N] f(\rho) d\rho \end{aligned} \quad (4.7)$$

where ρ is assumed constant over the block length and $f(\rho)$ is the probability density function (PDF) of ρ given by exponential density [23],

$$f(\rho) = \frac{1}{\bar{\rho}} \exp\left(-\frac{\rho}{\bar{\rho}}\right) \quad \rho \geq 0 \quad (4.8)$$

We have chosen here FH/FSK modulation scheme for the analysis of the MFRNET due to the inherent capability of the frequency hopping (FH) schemes to provide 'diversity' against frequency-selective fading encountered in mobile radio channel and the ability of FH/FSK scheme to accommodate more simultaneous users than other available schemes. Furthermore, of the two principal SS implementations - frequency hopping (FH) and direct sequence (DS), the FH systems can achieve much wider SS bandwidths resulting in higher processing gains, they generally use lower pseudonoise (PN) spreading code rates and noncoherent demodulation permitting faster link acquisition, they can hop around frequency bands that are unusually noisy or exhibit severe fading. On the other hand, DS spread spectrum system performs very poorly under multi-user interference and fading channel conditions.

The probability of bit error for FH/FSK in the presence of a partial-band noise interference is obtained as follows: A partial-band interference channel [24] is characterized by AWGN over only a fraction of the potential transmission bandwidth, but with the same average noise density. Let the total hopped bandwidth be W Hz and thermal noise (AWGN) be present over the entire hopped bandwidth of one-sided power spectral density (PSD) N_0 Watts/Hz. The partial-band noise interference is modeled as additional thermal noise over a fraction of the band, which is designated as c , $0 \leq c \leq 1$. The bandwidth of the partial-band interference is therefore cW Hz and its one-sided PSD is $N_{Jc} = J/cW$ Watts/Hz., where J is the average interference power. As the FH system hops, its carrier over the bandwidth W , there is a probability c that the effective PSD from all sources is $(N_0 + N_{Jc})$ and there is a probability $(1 - c)$ that the effective PSD is N_0 . Therefore, the probability of error for this system is given by,

$$P_b = c P_b \left[\left(\frac{E_b}{N_0 + N_{Jc}} \right)_{\text{eff.}} \right] + (1 - c) P_b \left(\frac{E_b}{N_0} \right) \quad (4.9)$$

where, $P_b \left(\frac{E_b}{N_0} \right)$ is the probability of error for ideal FSK given by,

$$P_b \left(\frac{E_b}{N_0} \right) = \frac{1}{2} \exp \left(- \frac{\frac{E_b}{N_0}}{2} \right) \quad (4.10)$$

and $P_b \left(\frac{E_b}{N_0 + N_{Jc}} \right)_{\text{eff.}}$ is the probability of error when the carrier is located within the bandwidth of the partial-band

noise interference. Within the region of partial-band interference,

$$\left(\frac{E_b}{N_0}\right)_{\text{eff.}} = \frac{E_b}{N_0 + N_{Ja}} = \left[\left(\frac{E_b}{N_0}\right)^{-1} + \left(\frac{E_b}{N_{Ja}}\right)^{-1} \right]^{-1} \quad (4.11)$$

We can write the SNR representing the interference as,

$$\left(\frac{E_p}{N_{Jc}}\right) = \frac{E_p}{J/cw} = a \left(\frac{E_p}{J/w}\right) = a \left(\frac{E_p}{N_J}\right) \quad (4.12)$$

when $a = 1$, the interference is over the entire FH bandwidth and the PSD of the interference is defined as $N_J = J/w$ Watts/Hz. Now let us assume that the thermal noise is sufficiently small, i.e.,

$$\frac{E_p}{N_c} \gg \frac{E_p}{N_J} \quad (4.13)$$

The probability of error for FH/FSK in the presence of partial-band noise interference given by equation (4.9) reduces to,

$$\begin{aligned} P_b &= a P_b \left[\left(\frac{E_b}{N_0}\right)_{\text{eff.}} \right] \\ &= \frac{c}{2} \exp \left[-\frac{1}{2} \left(\frac{E_p}{N_c}\right)_{\text{eff.}} \right] \\ &= \frac{c}{2} \exp \left[-\frac{c}{2} \left(\frac{E_p}{N_J}\right) \right] \quad (4.14) \end{aligned}$$

where (E_b/N_J) is the bit energy-to-interference density ratio and is denoted by ρ , and the probability of bit error P_b is denoted by $\epsilon(\rho)$.

Substituting equations (4.14) and (4.8) into equation (4.7) yields

$$\bar{P}_{be} = \frac{1}{\bar{\rho}} \int_0^{\infty} [1 - [1 - \frac{\alpha}{2} \exp(-\frac{\alpha}{2}\rho)]^N] \exp(-\frac{\rho}{\bar{\rho}}) d\rho \quad (4.15)$$

For large N and general values of $\bar{\rho}$, we can approximate

$$g(\rho) = 1 - [1 - \epsilon(\rho)]^N$$

by a step function leading to,

$$\bar{P}_{be} = \int_0^{\rho'} g(\rho) d\rho = F(\rho') \quad (4.16)$$

Thus probability of block error averaged over the fading signal level \bar{P}_{be} is approximated by the cumulative distribution function (CDF) of ρ evaluated at some point $\rho = \rho'$ where ρ' is chosen as $\rho' = \rho_0$, which is obtained by requiring the equality between the integral of $g(\rho)$ and the integral of its approximation. Therefore, for Rayleigh fading, the step function approximation for \bar{P}_{be} is,

$$\bar{P}_{be} = F(\rho_0) = 1 - e^{-\rho_0/\bar{\rho}} \quad (4.17)$$

where,

$$\begin{aligned}
 \rho_0 &= \int_0^{\infty} g(\rho) d\rho \\
 &= \int_0^{\infty} \left[1 - \left[1 - \frac{a}{2} \exp\left(-\frac{a}{2}\rho\right) \right]^N \right] d\rho \\
 &= \frac{2}{a} \int_0^{\infty} \left[1 - \left[1 - \frac{a}{2} \exp(-x) \right]^N \right] dx \quad (4.18)
 \end{aligned}$$

This expression is computed numerically for $a=0.5$ and $a=0.1$. Hence the dynamic block error probability \bar{P}_{be} can be computed from equation (4.17) for a given average SNR $\bar{\rho}$.

4.3 NUMERICAL RESULTS AND SYSTEM PERFORMANCE

The performance of the nonpersistent CSMA/CD in mobile packet radio channel degraded with slow Rayleigh fading was derived for FH/FSK modulation scheme in Section 4.1. Also, the average probability of block error was derived in Section 4.2, which gives the probability of packet error and the probability of ACK error due to imperfect or unreliable channel, as we are considering blocked data transmission over random channels.

Consider a 1000-bit packet ($N_p = 1000$), a 100-bit acknowledgement ($N_a = 100$) and equal bit energy-to-noise density ratios (i.e. $\bar{E}_p = \bar{E}_a = \bar{E}$). Numerical computation of equation (4.18) yields,

For $a=0.5$:

$$\left. \begin{aligned} \rho_0(N_p) &= 24.352 \\ \rho_0(N_e) &= 15.2 \end{aligned} \right\} \quad (4.19)$$

For $a=0.1$:

$$\left. \begin{aligned} \rho_0(N_p) &= 89.74 \\ \rho_0(N_e) &= 43.84 \end{aligned} \right\} \quad (4.20)$$

The channel throughput given by equation (4.5) takes the following form after substituting for the probabilities F_{pe} and F_{ee} from equation (4.17),

$$S = \left(\frac{\Gamma_2 G e^{-2G}}{\Gamma_2 G e^{-2G} + (1 - e^{-2G} - 2G e^{-2G}) \gamma - 1} \right) (e^{-\rho_0/\bar{\rho}_p}) (e^{-\rho_0/\bar{\rho}_e})$$

$$= \left(\frac{\Gamma_2 G e^{-2G}}{\Gamma_2 G e^{-2G} + (1 - e^{-2G} - 2G e^{-2G}) \gamma - 1} \right) \exp \left[\frac{-\rho_0(N_p) - \rho_0(N_e)}{\bar{\rho}} \right] \quad (4.21)$$

Invoking equations (4.19) and (4.20) here we obtain,

For $a=0.5$,

$$S = \left(\frac{\Gamma_2 G}{\Gamma_2 G e^{-2G} + (1 - e^{-2G} - 2G e^{-2G}) \gamma - 1} \right) \exp \left[-2G - \frac{39.552}{\bar{\rho}} \right] \quad (4.22)$$

For $a=0.1$,

$$S = \left(\frac{\Gamma_2 G}{\Gamma_2 G e^{-2G} + (1 - e^{-2G} - 2G e^{-2G}) \gamma - 1} \right) \exp \left[-2G - \frac{133.58}{\bar{\rho}} \right] \quad (4.23)$$

The throughput equations given by (4.22) and (4.23) are derived using step function approximation for large block

sizes. A comparison of the exact and approximate result shows an excellent agreement.

Figure (4.1) shows the (S,G) relationship for CSMA-CD in FH/FSK mobile packet radio. This figure exhibits improvement in channel capacity gained by CSMA-CD over the CSMA scheme [18]. For random access schemes, in general, the fact that throughput(S) drops to zero as the offered channel traffic (G) increases indefinitely is indicative of unstable behavior [25]. However, we notice that CSMA-CD can maintain a throughput relatively high and near capacity over a very large range of the offered channel traffic in a mobile packet radio environment too. This suggests that CSMA-CD may not be as unstable as the other schemes, therefore, in the absence of dynamic control, it is capable of sustaining proper behavior even when the channel load exceeds that for which the system has been optimized.

It is noticed that higher throughput results for larger values of SNR and at about 40dB and above the conventional value of 0.96 is achieved (See Table .1). In Figure (4.2) similar relationship is shown for different value of the parameter c , defined as the fraction of the band over which partial-band noise interference exists. Better throughput performance is obtained for $c = 0.5$ and a sacrifice of 5dB is required if we choose $c = 0.1$. Furthermore, $c = 1$ corresponds to the ideal

FSK case in which interference is over the entire FH bandwidth.

We know that [26] CSMA-CD provides an improvement over CSMA both in terms of channel capacity and throughput-delay characteristics. Figures (4.3) and (4.4) show the sensitivity of this improvement to the packet length T and the collision detect time γ . The larger T gives better CSMA-CD performance for fixed γ . From Figure (4.3), we notice that the channel capacity increases from 0.018 at 10dB to 0.926 at 30dB SNR. Also, higher α gives better channel capacity performance. In Figure (4.4), we plot the channel capacity for the nonpersistent CSMA-CD versus γ for various SNR keeping fixed T . Higher channel capacity is obtained for lower γ and higher SNR again. Best performance is achieved for $\gamma = 2$ and SNR = 30dB, in that it gives channel capacity close to that obtained for stationary packet radio before [22]. Also, Tables 4.1 and 4.2 summarize these numerical values for larger range of parameters involved.

4.4 CONCLUSIONS

We modified the model used in the analysis of CSMA-CD to the case of mobile packet radio channel. It was shown that the throughput is sensitive to the SNR at the receiving node and at about 40dB the throughput performance close to the conventional CSMA-CD is obtained. The throughput degradation is severe at lower SNR values, say 10 dB. Therefore, to obtain a satisfactory performance of FH/FSK MPRNET and

gain all the advantages of the nonpersistent CSMA-CD scheme, it is desirable to have SNR at least 30 dB or so. Furthermore, CSMA-CD for MPRNET is more stable than CSMA, in that with the former the channel capacity and packet delay are less sensitive to variations in the average retransmission delay. Just as the CSMA (due to its carrier sensing capability before transmission) gives improved performance over slotted ALOHA, the CSMA-CD (due to its collision detection capability during transmission) gives improved performance over CSMA. The most interesting conclusion was that the SNR becomes a critical parameter in the performance evaluation of the CSMA-CD protocol in a FH/FSK spread spectrum mobile packet radio network.

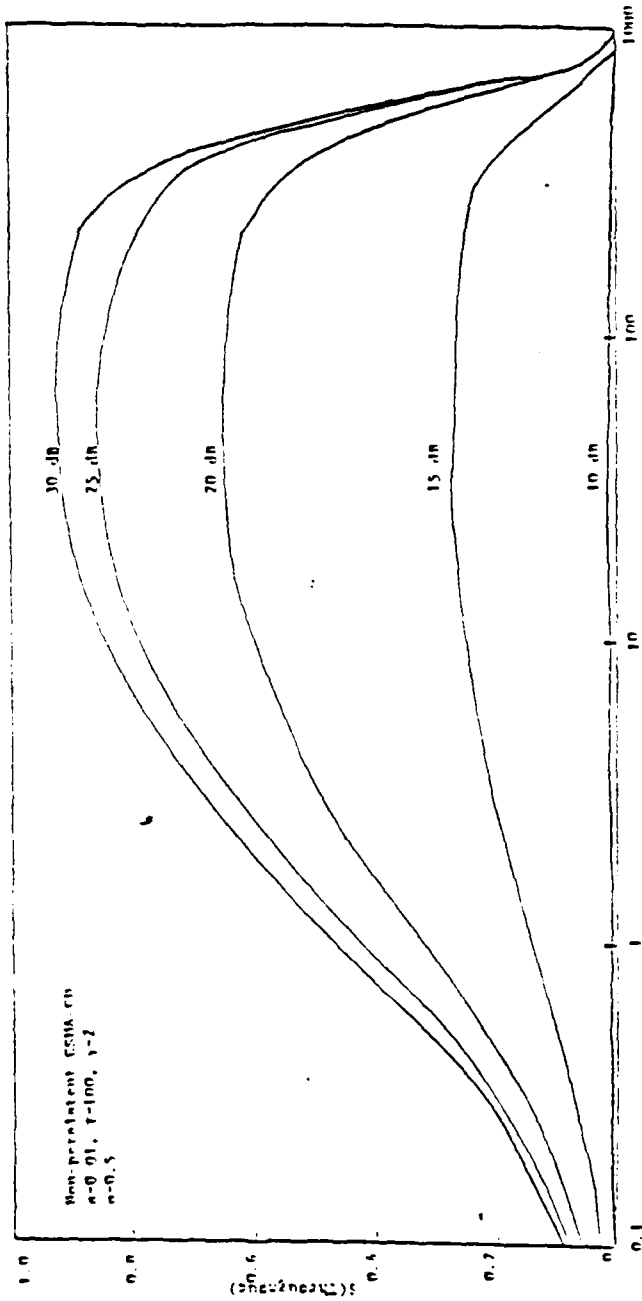


Figure 4.1 Throughput versus channel traffic for various dB and $\alpha=0.01$.

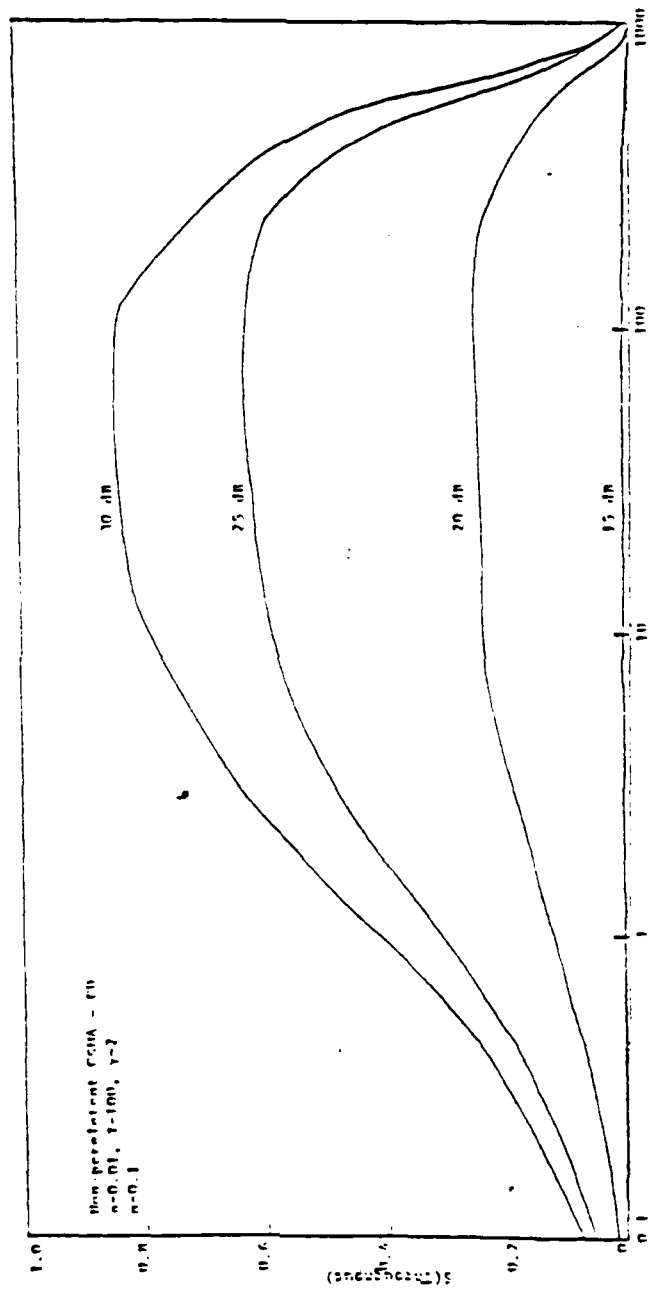


Figure 4. Throughput Versus Channel Traffic for Various dB and $\alpha=0.1$

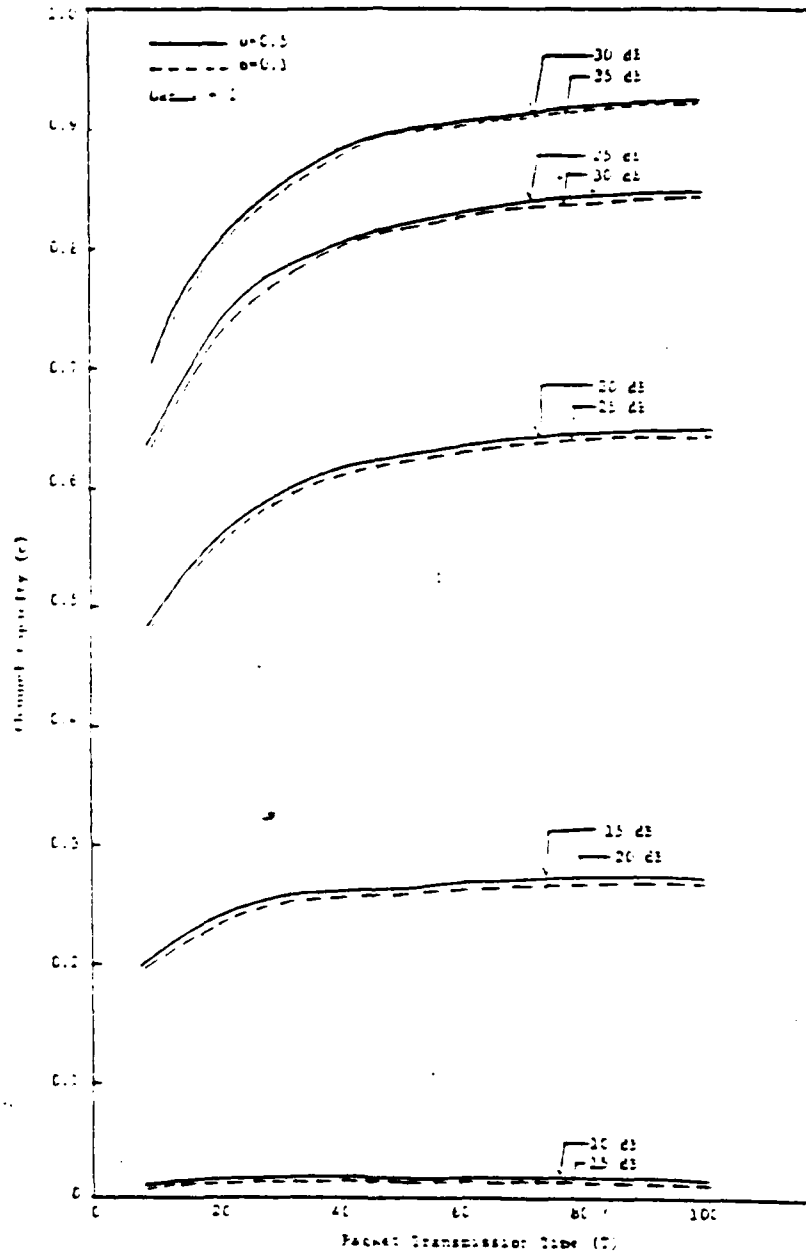


Figure 4.3 Channel Capacity versus packet transmission time at non-persistent CSMA/CD at three T.

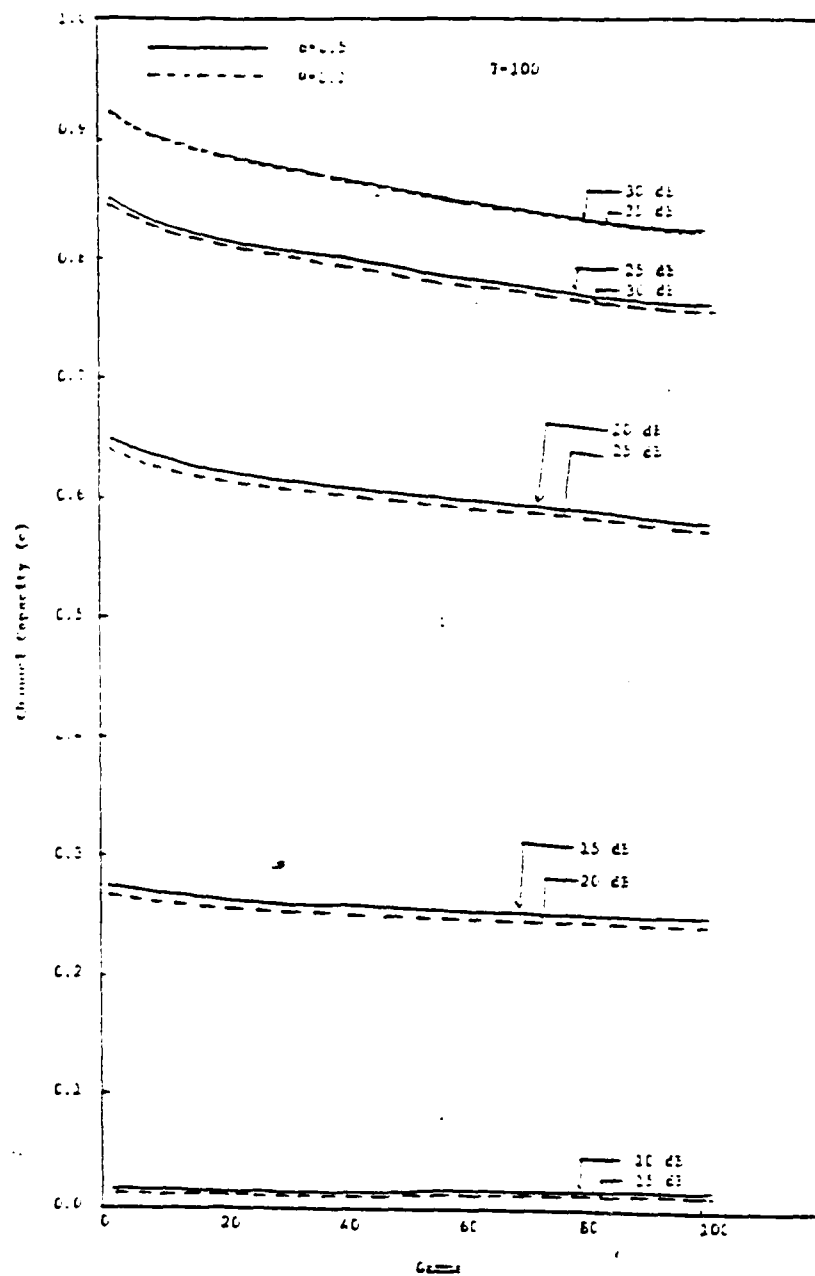


Figure 4.4 Channel capacity versus γ in non-persistent CSMA-CD at fixed packet length.

TABLE 4.1 Channel Capacity Variations with SNR and Packet Length T for a Fixed Gamma.

SNR P (dB)	Channel Capacity (C)											
	T = 10											
	p=0.5		p=0.1		p=0.5		p=0.1		p=0.5		p=0.1	
10	.014	—	.016	—	.018	—	.018	—	.018	—	.018	—
15	.208	.021	.241	.015	.262	.023	.269	.034	.273	.034	.276	.034
20	.489	.191	.566	.221	.615	.240	.633	.247	.643	.251	.649	.252
25	.641	.476	.741	.551	.806	.599	.830	.617	.843	.626	.849	.627
30	.698	.631	.809	.736	.878	.800	.904	.823	.918	.831	.924	.833
35	.717	.696	.831	.806	.901	.876	.929	.901	.943	.921	.937	.924
40	.723	.716	.838	.830	.910	.902	.937	.928	.951	.940	.946	.937
45	.725	.723	.840	.834	.913	.910	.940	.937	.954	.951	.951	.949
50	.726	.725	.841	.840	.913	.913	.940	.940	.955	.954	.953	.952

TABLE 4.2 Channel Capacity Variations with SNR and Gamma for a Fixed Packet Length.

SNR P (dB)	Channel Capacity (C)													
	T = 100													
	p=0.5		p=0.1		p=0.5		p=0.1		p=0.5		p=0.1		p=0.5	
10	.018	—	.018	—	.018	—	.017	—	.017	—	.017	—	.017	—
15	.276	.014	.270	.014	.266	.014	.259	.013	.254	.013	.250	.013	.244	.013
20	.649	.253	.623	.244	.624	.244	.610	.238	.598	.234	.587	.229	.576	.224
25	.850	.631	.831	.618	.818	.608	.794	.594	.764	.581	.730	.570	.704	.554
30	.926	.843	.907	.825	.892	.813	.871	.793	.854	.779	.839	.763	.827	.753
35	.951	.924	.921	.904	.916	.899	.899	.888	.878	.868	.851	.841	.830	.820
40	.960	.951	.939	.931	.924	.915	.902	.894	.883	.877	.869	.861	.850	.844
45	.961	.960	.942	.936	.926	.924	.904	.902	.889	.884	.872	.864	.854	.847
50	.961	.961	.943	.947	.927	.926	.906	.905	.889	.887	.872	.871	.861	.854

CHAPTER V

BANDWIDTH EFFICIENT DIGITAL MODULATIONS FOR MOBILE RADIOS

Improving the capacity of Cellular Mobile Radio System calls for bandwidth efficient Digital Modulation and bit rate efficient Speech Coding techniques. Though Spread Spectrum schemes received considerable interest recently, formidable technological problems and questionable cost effectiveness have prompted investigation of conventional Digital Modulation schemes. In this chapter we review a class of spectrally efficient modulation schemes employing simple receivers. A speech transmission scheme using these modulations and DPCM coding is considered in the next chapter.

5.1. INTRODUCTION

The ever increasing demand for radio frequency spectrum has led to a wide variety of techniques for solving the problem of spectral congestion. Spectrally efficient modulation systems has received considerable interest in this respect. Even though the primary objective of spectrally efficient modulation is to maximize the bandwidth efficiency, the scheme should achieve this at a prescribed average bit error rate with minimum expenditure of signal power. The desirability of constant envelope modulation, in addition to good error performance, has led to a class of Phase Modulation.

Continuous Phase Modulation (CPM) has received considerable attention recently. It is seen that by making the phase continuous the spectral behaviour and performance can be improved. Further improvement in spectra can be obtained by introducing memory into the system. Such schemes known as Partial Response CPM introduce controlled intersymbol interference to improve the spectral behaviour. The spectral improvement takes place without increase in probability of error at practical SNR, but the price to be paid is the system complexity especially with respect to the optimum receivers. However, simple sub-optimum receivers are found to yield very good performance in special cases.

5.2 TRANSMITTER AND RECEIVER PRINCIPLES

5.2.1 Modulation Schemes

The modulation schemes considered in this work belong to a class of constant amplitude, Partial Response CPM.

Let ... $\alpha_{n-2}, \alpha_{n-1}, \alpha_n, \alpha_{n+1}, \alpha_{n+2} \dots$ be an infinite sequence of statistically independent binary data symbols taking values ± 1 with equal probability. The transmitted signal is of the form

$$s(t, \underline{\alpha}) = \sqrt{(2E/T)} \cos [2\pi f_0 t + \phi(t, \underline{\alpha}) + \phi_0] \quad (5.1)$$

where the information carrying phase is

$$\phi(t, \underline{\alpha}) = 2\pi h \int_{-\infty}^{\infty} \alpha_i g(t-iT) \quad (5.2)$$

where E is the symbol energy, T is the symbol time, f_0 is the carrier frequency, and h is the modulation index. For coherent transmission and reception the arbitrary phase ϕ_0 can be set to zero. The phase response $g(t)$ is defined by

$$g(t) = \int_{-\infty}^t g(\tau) d\tau \quad (5.3)$$

where $g(t)$ is the frequency response pulse. The frequency pulse is time-limited.

$$g(t) = 0 \quad t < L_1 T, \quad t > L_2 T \quad (5.4)$$

where $L = (L_1 - L_2)T$ is the duration of the frequency pulse and

$$\int_{L_1 T}^{L_2 T} g(t) dt = 1/2 \quad (5.5)$$

For details, refer to [27] - [29]

For $nT \leq t \leq (n+1)T$, the information carrying phase is given by

$$\phi(t, \alpha_n) = 2\pi h \sum_{i=-\infty}^{n-L_1} \alpha_i q(t-iT) \quad (5.6)$$

At any time $t = nT$, the information carrying phase can be seen as an intersymbol interference (ISI) around the phase node θ_n . The introduction of this controlled intersymbol interference results in improved spectral behaviour. Define the phase node

$$\theta_n = h\pi \sum_{i < n-1} \alpha_i \quad (5.7)$$

We see that α_n can be determined by

$$\alpha_n = (1/h\pi) (\theta_{n+1} - \theta_n) \quad (5.8)$$

The phase ambiguity can be resolved by differential encoding [30].

The modulations considered in this paper have the pulse shapes given by

Minimum Shift Keying (MSK)

$$g(t) = \begin{cases} 1/2T & 0 \leq t \leq T \\ 0 & \text{otherwise} \end{cases} \quad (5.9)$$

The Raised Cosine scheme (RC)

$$g(t) = \begin{cases} (1/2LT) \{1 - \cos(2\pi t/LT)\} & 0 \leq t \leq LT \\ 0 & \text{otherwise} \end{cases} \quad (5.10)$$

5.2.2 Receivers

The optimum receivers for the partial response CPM based on the Viterbi Algorithm is often complex. But for binary schemes with modulation index $h = 1/2$ simple sub-optimum receivers of the modified offset quadrature type yield good results. They can be constructed with only two filters and simple decision logic. The receiver structure is shown in Figure 5.1. The filters are normally identical and the decision logic consists of a delay and logic for differential decoding. The optimum receiver filter in this class is given by [31]

$$a(t) = \sum_{j=1}^{m/2} a_j s(t, \underline{\alpha}_j^+) \quad (5.11)$$

where $s(t, \underline{\alpha}_j^+)$ is the signal corresponding to the transmitted sequence j in the subset having $s(t_0, \underline{\alpha}) > 0$, where t_0 is the time when the decision is made, and a_j , $j = 1, 2, \dots, m/2$, should be chosen to minimize the probability of error. $m = 2^{N+L-1}$ is the number of different transmitted sequences for a receiver filter of duration NT .

We consider three different types of receiver filters. The optimum filter for very small SNR, the averaged matched filter (AMF), is given by [31]

$$a(t) = \frac{2}{m} \sum_{j=1}^{m/2} s(t, \underline{\alpha}_j^+) \quad (5.12)$$

The optimum filter for large SNR, the asymptotically optimum filter (AOF), given in reference [31] belongs to the MSK-type receivers and is analysed.

Another filter considered is the MSK filter in the receiver given by

$$a(t) = \begin{cases} \sin(\pi t/2T) & 0 \leq t \leq 2T \\ 0 & \text{otherwise} \end{cases} \quad (5.13)$$

5.3 PERFORMANCE

The phase node is estimated by observing the output of the cosine and sine channel at every odd and even symbol intervals. This means that decisions are made alternatively from the two quadrature arms. For any given data sequence, the decision after the filter is a comparison between a Gaussian random variable and a threshold which is zero. Therefore the mean and variance of the random variable determine the error probability. Assuming that s_j^+ is transmitted, the mean value

$$\lambda_j = \langle s_j^+, a \rangle \quad (5.14)$$

where $\langle \rangle$ is the inner product in the Eculidean space. The variance σ^2 is independent of any particular signal and is given by

$$\sigma^2 = \frac{T}{E} \frac{N_0}{2} |a|^2 \quad (5.15)$$

where N is the one sided spectral density of additive white Gaussian noise. Since the mean of the output of the filter depends on the transmittd sequence, the probability of error can be expressed in terms of the squared Eculidean distance defined as

$$d_j^2 = \frac{2}{T} \frac{[\langle s_j^+, a \rangle]^2}{|a|^2} \quad (5.16)$$

The error rate in estimating the phase node sequence ϵ_n is then calculated by averaging over all possible transmitted sequences, as a function of signal to noise ratio.

$$P = \frac{1}{m} \sum_{j=1}^m Q(\sqrt{d_j^2 E/N_0}) \quad (5.17)$$

where $Q(x)$ is the Gaussian error function

$$Q(x) = \frac{1}{\sqrt{2\pi}} \int_x^{\infty} e^{-y^2/2} dy \quad (5.18)$$

Figure 5.2 gives the error probability in detecting the phase node for MSK, 2RC, 3RC, 4RC and TFM schemes using MSK filters. Reference [29] gives more exhaustive results for other types of filters. With differential encoding to resolve the relationship between phase nodes and data symbols, the bit error probability P is given by

$$P_e \approx 2 P_{\theta} (1 - P_{\theta}) \quad (5.19)$$

5.4. DISCUSSIONS

A class of spectrally efficient modulations and simple sub-optimum receivers have been considered for application to cellular mobile radios. The simple receivers belong to the Modified Offset Quadrature receivers (MSK type). Error performance curves show that bandwidth efficient schemes can be used with MSK type receivers with an asymptotic loss less than 1 dB compared to MSK. The loss at intermediate error probability is even smaller. The drawback of the receiver is that it can be used only for binary signalling with $h = 1/2$ CPM schemes. Many of the interesting schemes are however in this class.

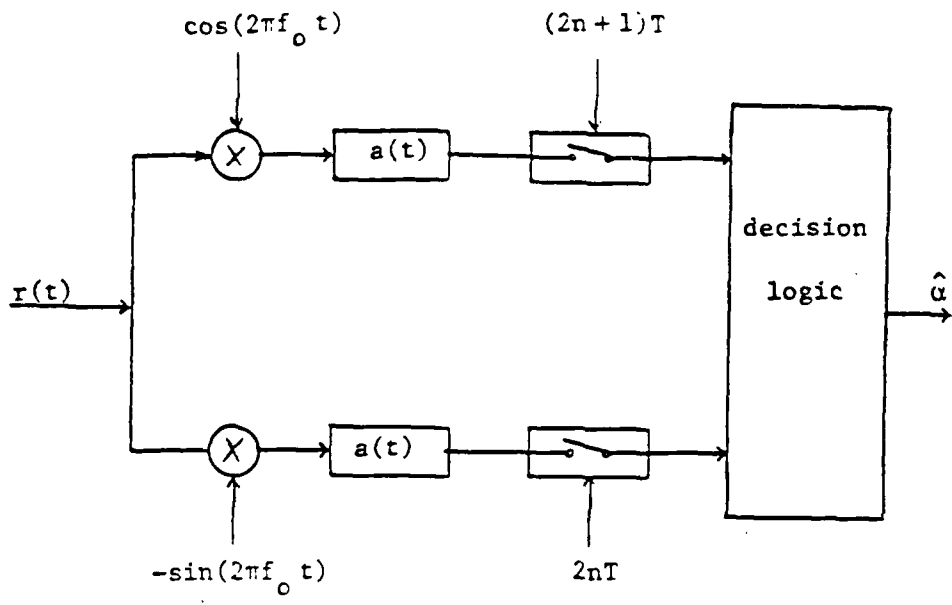


Figure 5.1 Receiver structure for MSK type receivers for partial response CPM.

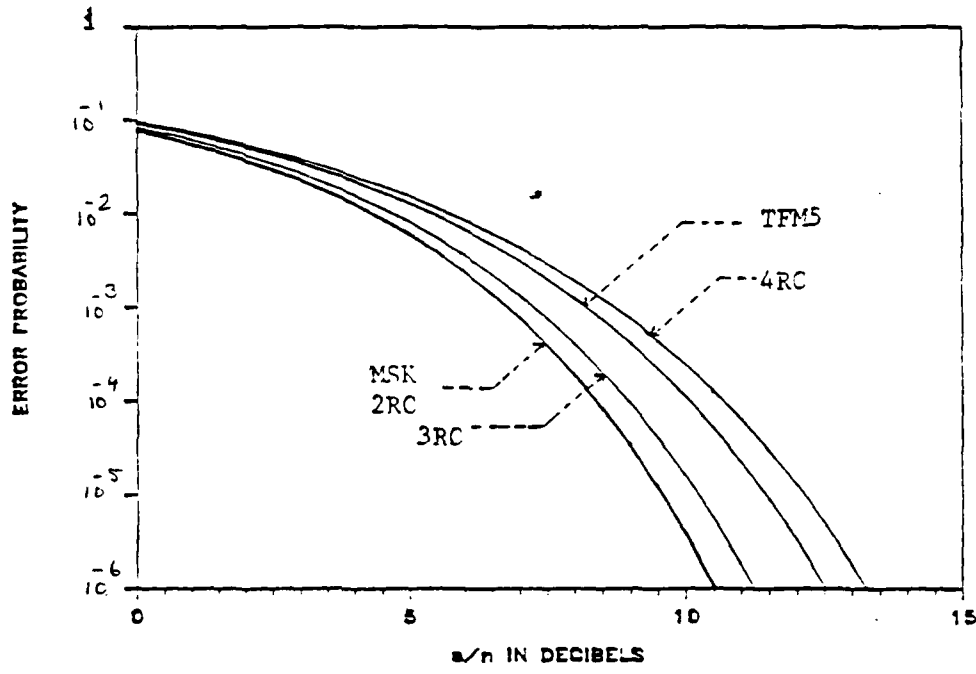


Figure 5.2 Error probability in detecting the phase node sequence for various binary, $h = \frac{1}{2}$, schemes (MSK filter).

CHAPTER VI

SPEECH TRANSMISSION USING DPCM CODING PARTIAL RESPONSE CPM AND DIVERSITY

In this chapter, we consider the performance of a speech transmission scheme using DPCM coding and Partial Response Continuous Phase Modulation. The performance measure is the audio signal to noise ratio. Both quantizing noise and transmission errors contribute to the overall mean-square error. It is seen that in a fading environment space diversity is very effective in bringing down the threshold of channel signal to noise ratio to maintain the audio signal to noise. The number of channels the systems can support is evaluated under various conditions.

6.1 INTRODUCTION

Recent developments in speech digitization have prompted an examination of digital coding as a possibility for mobile radio. The greater bandwidth demanded by the digital representation can be overcome by bit rate efficient speech coding schemes. In mobile radio environments characterized by large error rates the effect of transmission errors in speech coding schemes have received considerable interest. However, for complex coding schemes, the study has been limited to simulations. The effect of channel errors in embedded DPCM has been analyzed and found to be suitable for variable bit rate transmission under Gaussian and Rayleigh fading conditions.

Mobile radio channel which suffers from severe multipath fading results in unacceptably high error rates. Channel coding has been suggested as a possibility to combat high error rates. Fading can also be combated with space diversity without expending additional bandwidth. Withtime division

retransmission (TDR) mobile unit can be kept simple at the same time several branches of diversity can be assured providing a reasonable error rate in the fading channel.

In this chapter we consider the performance of a speech transmission scheme using DPCM coding, partial response CPM and diversity over Rayleigh fading channel in additive white Gaussian noise. Base to mobile transmission with three cells per cluster and seven cells per cluster is considered. Centrally located base station with omni-directional antenna is assumed. Co-channel interference is assumed to be the main cause of interference. A recent investigation on the performance of Partial Response CPM with MSK receiver shows that, for the signal to co-channel interference ratio encountered in mobile radio channels, the adjacent channel interference is negligible even when the spectra are allowed to overlap partially [32]. Hence the capacity of the cellular mobile radio system can be improved by allowing the spectra of the adjacent channels to overlap partially, without significant degradation in performance.

6.2 FADING AND DIVERSITY COMBINING

Two major impairments of mobile radio communication systems are interference from other users and multipath fading. Interference among users results from the frequency re-use designed to increase the capacity of the system. Each cell in a cellular system is assigned a number of channels in a frequency division system. The same set of frequencies is reused at a cell further away. This results in mutual interference between the users. The signal to co-channel interference ratio is affected by the re-use factor, the base station location, signal attenuation factor and the antenna configuration.

For digital transmission over fading channels the time variations of the signal to noise ratio (s/n) results in a changing error probability. This leads to clustering of errors and increased average probability of error. Bit scrambling prior to transmission assures random occurrence of error patterns. We assume slow Rayleigh fading where the time varying s/n is approximately constant over several transmitted bits. The density function for the signal to noise ratio is

$$f(\gamma) = (1/\Gamma) \exp(-\gamma/\Gamma) \quad (6.1)$$

where Γ is the average signal to noise ratio. The average error probability for the fading case is given by

$$P = \int_0^{\infty} f(\gamma) P_e(\gamma) d\gamma \quad (6.2)$$

where $P_e(\gamma)$ is the average error probability of the modulation scheme for Gaussian noise at the s/n γ . The increased probability of error can be combated using diversity. For maximal ratio combining the error probability of coherent MSK type detection of partial response CPM signals is [33]

$$P = \frac{1}{2\pi} \prod_{j=1}^M \left[1 - \frac{\sqrt{d_j^2 \Gamma/2}}{\sqrt{1+d_j^2 \Gamma/2}} \left\{ 1 + \frac{1}{1+2} \left(1 + \frac{d_j^2 \Gamma}{2} \right)^{-1} + \dots + \frac{1.3.5 \dots (2M-3)}{(M-1)! 2^{M-1}} \left(1 + \frac{d_j^2 \Gamma}{2} \right)^{-(M-1)} \right\} \right] \quad (6.3)$$

where Γ is the average per branch s/n and M is the number of diversity branches. For selection combining the error probability is given by [33]

$$P = \frac{1}{2\pi} \prod_{j=1}^M \sum_{k=0}^{M-j} \frac{(-1)^k \binom{M-j}{k}}{\sqrt{1 + (2k/d_j^2) \Gamma}} \quad (6.4)$$

Space diversity is commonly employed in mobile radios to combat fading without the need for additional bandwidth. With time division retransmission all diversity combining takes place at the base station. The equipment at the mobile can be kept simple and at the same time several branches of diversity can be assured. The use of frequency offset reference transmission for improved reference signal to interference ratio [34] can be employed, with slight modification, even when the adjacent channel spectra overlaps partially.

Base to mobile transmission with centrally located base station and omni-directional antenna is considered in this work. The worst case signal to co-channel interference for a three cell cluster for the above base station and antenna configuration is 5.1 dB [35]. Following calculations similar to that in [35], the worst case signal to co-channel interference for a seven cell cluster yields 11.5 dB. The signal attenuation is assumed to follow inverse cubic law in the signal to co-channel interference ratio calculations. The co-channel interference is modelled as stationary white Gaussian noise with power spectral density $N_0/2$ and is assumed to be the main cause of interference. It is also assumed that fading of the total interference is negligible compared to the fading of the signal.

SOURCE CODERS

The source coder considered in this paper is embedded

DPCM operating at 32 k.b.p.s. Both quantizing noise and digital noise due to transmission errors contribute to the overall output mean squared error. Reference [36] presents a detailed analysis of the transmission errors in embedded DPCM. The output signal to noise ratio is given in the form

$$s/n = E\{x(k)\}^2 / E\{x'(k) - x(k)\}^2 \quad (6.5)$$

where $x(k)$ and $x'(k)$ are the encoder input and decoder output respectively. The above reduces to

$$s/n = \frac{C_{\text{source}}}{c_q^2 + c_{qt}^2} \quad (6.6)$$

where C_{source} is a constant and depends on the codec configuration and source statistics, c_q^2 is the quantising noise power and c_{qt}^2 is the distortion due to transmission errors including the effects of correlation between quantizing noise and noise due to transmission errors. With single integration DPCM and 2 bit minimal quantizer [37]

$$C_{\text{source}} = \frac{1 - a^2 L_c^2 / 48}{L_q^2 (1 - 2a\rho + a^2)} \quad (6.7)$$

where a is the predictor coefficient of the DPCM feedback loop, ρ is the adjacent sample autocorrelation and L_q is the quantizer overload factor.

$$c_q^2 \approx 2^{-2D} / 3 \quad (6.8)$$

and

$$C_{qt}^2 = P[\tilde{T}_1(D) + b T_1(M)] + P^2[\tilde{T}_2(D) + b T_2(M)] \quad (6.9)$$

where

$$b = a^2 / (1 - a^2) \quad (6.10)$$

and P is the probability of bit error. $\tilde{T}_1, \tilde{T}_2, T_1, T_2$ are constants associated with input statistics, overload factor, binary representation and transmission format, D is the transmission rate per sample and M is the minimum bit rate per sample of the transmission system. For embedded DPCM with $D=4$ and $M=2$, an overload factor $\sqrt{10}$, Gauss-Markov input in sign-magnitude representation, we have, for uncoded transmission [36]

$$C_{source} = 0.3056 \quad (6.11)$$

$$C_{qt}^2 = P(0.723 + 0.725b) + P^2(0.271 + 0.275b) \quad (6.12)$$

Evaluation of the embedded DPCM using computer simulation technique over Gaussian and Rayleigh fading channels resulted in close agreement between the computed audio s/n and simulated segmental signal to noise ratio [37]. This motivates the use of audio s/n as a measure of performance in comparing various schemes in the next section.

NUMERICAL RESULTS.

Audio signal to noise ratio is computed as a function of channel s/n for various modulation schemes considered in

this paper. The source coder is embedded DPCM with transmission rate 4 bits per sample and minimum bit rate 2 bits per sample. A Gauss Markov input signal with adjacent sample correlation of 0.85 is assumed. The codec uses single integration with coefficient $a = 0.85$ and a load factor $L_q = \sqrt{10}$. Formulas given in sections III and IV are used to compute the probability of error and audio signal to noise ratio.

Figure 6.1 shows audio s/n as a function of channel s/n in a non-fading channel for MSK, 2RC, 3RC, TFM5, and 4RC schemes. Figure 6.2 shows the corresponding plots for a fading channel without diversity. Curves are shown only for MSK and TFM5. The relative positions of 2RC, 3RC and 4RC are retained.

Figures 6.3 to 6.5 show the audio s/n versus average per branch s/n for an increasing number of diversity branches with maximal ratio combining. Figure 6.6 shows the corresponding plot for 2 branch selection combining.

DISCUSSION AND CONCLUSIONS.

This chapter considers space diversity as an alternative to channel coding treated in Reference [36], to extend the threshold of channel s/n for maintaining the audio s/n in a fading environment, for various modulation schemes considered. Diversity is used with and without time division retransmission. In the following discussion we evaluate the number of channels that can be supported by the available bandwidth of 40 M.Hz.

It can be seen from Figure 6.1 that in a non-fading channel an s/n of 10 dB is required for an audio s/n of 20 dB. The very large channel s/n required to maintain an adequate audio s/n in a fading environment is evident from Figure 6.2. Considering the average signal to noise ratio encountered in mobile radio environment it is clear that some form of diversity should be employed to bring down the threshold of channel s/n without sacrificing the audio s/n. A three cell cluster has an average channel s/n of 5.1 dB. A 4 branch maximal ratio combining yields an audio s/n of 19 dB for MSK and 15.5 dB for 4RC, with 2RC, 3RC, and TFM5 in between. An 8 branch diversity with maximal ratio combining yields over 23 dB audio s/n for all the modulation schemes considered.

Since more than 2 diversity branches is inconvenient on a mobile, time division retransmission is to be employed. To achieve 32 k.b.p.s in each direction a symbol rate of 81 kbaud is required [35]. (the overhead over 64 k.b.p.s. is due to the co-phasing procedure for the TDR scheme.) With a channel spacing of 64 KHz, a bit rate to frequency spacing ratio of 0.79, 208 two way channels are possible.

If we consider schemes without TDR and a 2 branch diversity it is necessary to consider a larger frequency reuse factor. For a seven cell cluster the average per branch s/n is 11.5 dB. With 2 branch maximal ratio combining this yields an audio s/n of 17 dB to 15 dB depending on the

modulation scheme. With 2 branch selection combining the corresponding figure is 15 dB to 13 dB. Employing 28 KHz channel spacing, a bit rate to frequency spacing ratio of 0.875, this results in about 102 channels.

From the numerical results and discussion above it is seen that a large number of channels can be provided in a digital mobile radio system by the proper combination of speech coding schemes, bandwidth efficient modulation schemes, diversity and time division retransmission. Base station and antenna configuration, channel coding and more efficient speech coding schemes can further extend the capacity of the system.

Throughout the discussion we have considered idealized conditions of transmission and reception. Perfect timing and synchronization were assumed with coherent detection and ideal diversity combining. The performance depends highly on the above assumptions.

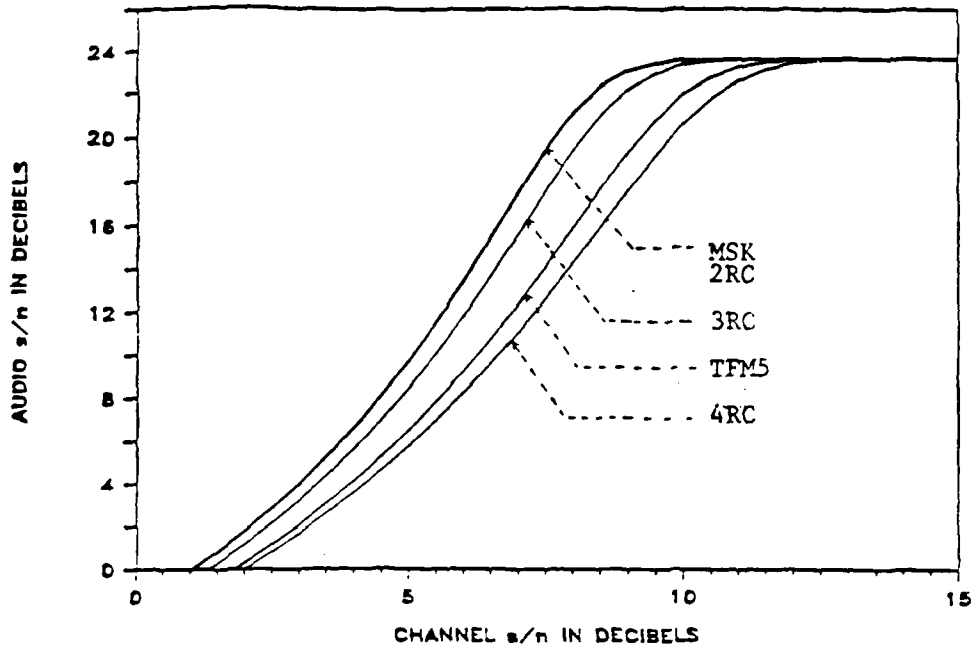


Figure 6.1 Performance of the speech transmission scheme for various modulation schemes in non-fading channel

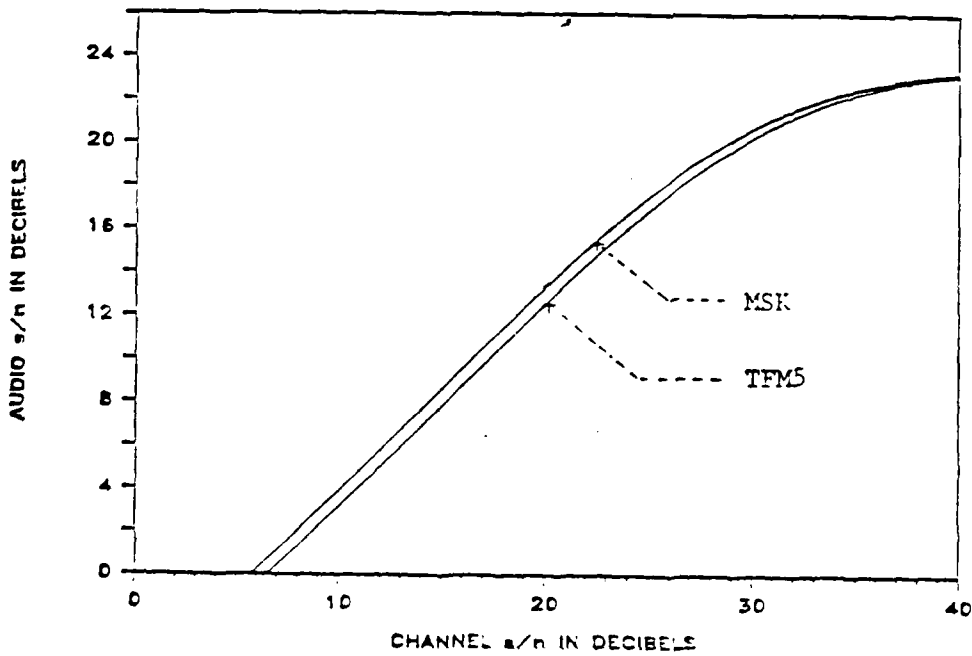


Figure 6.2 Performance of the speech transmission scheme for MSK and TFMS modulation schemes in Rayleigh fading channel.

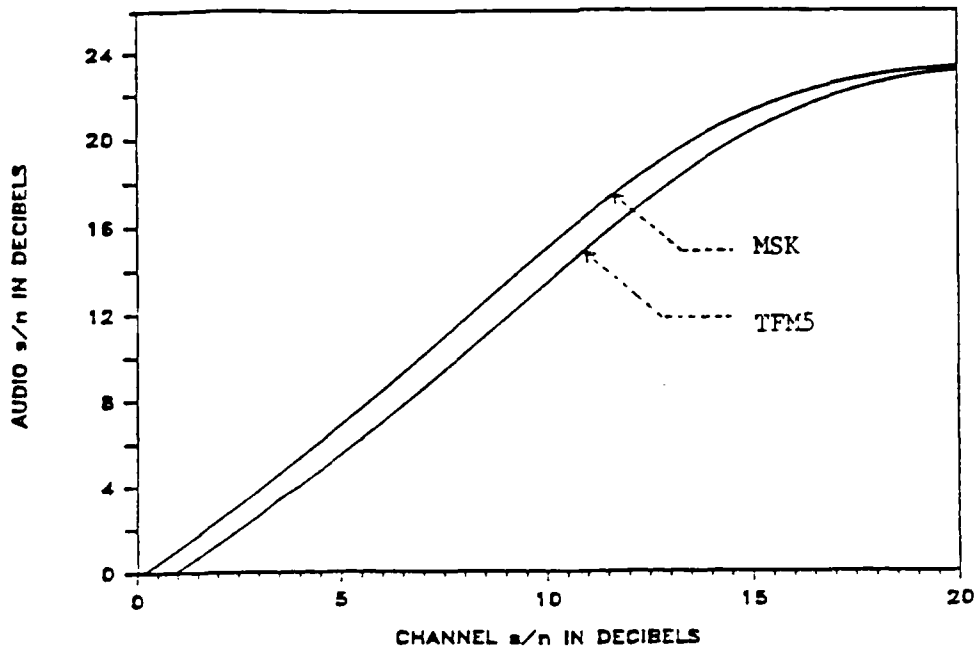


Figure 6.3 Performance of the speech transmission scheme for MSK and TFM5 modulation schemes in Rayleigh fading channel with 2 branch maximal ratio combining.

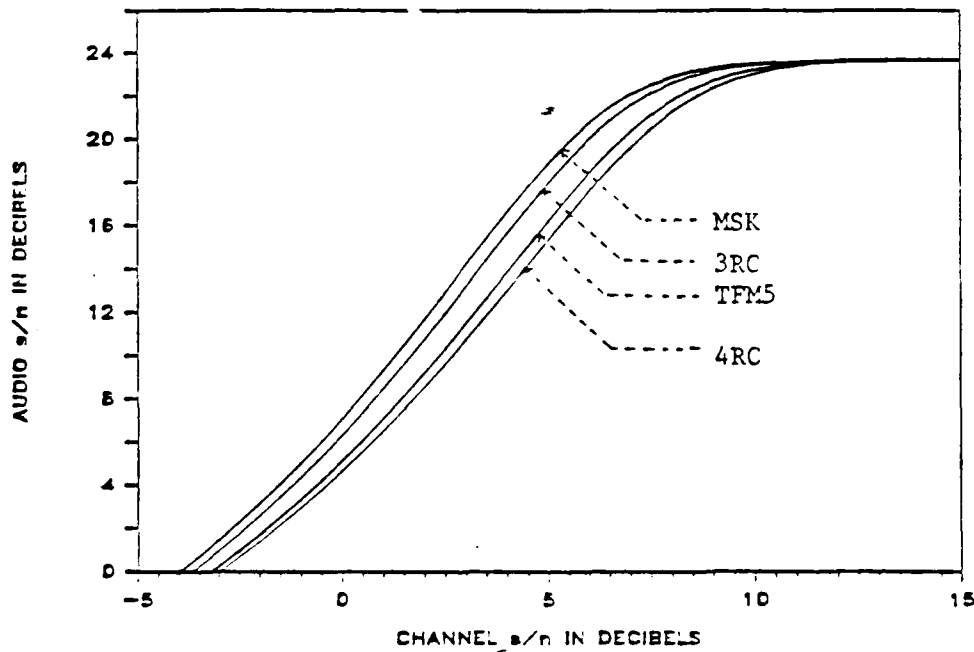


Figure 6.4 Performance of the speech transmission scheme for various modulation schemes in Rayleigh fading channel with 4 branch maximal ratio combining.

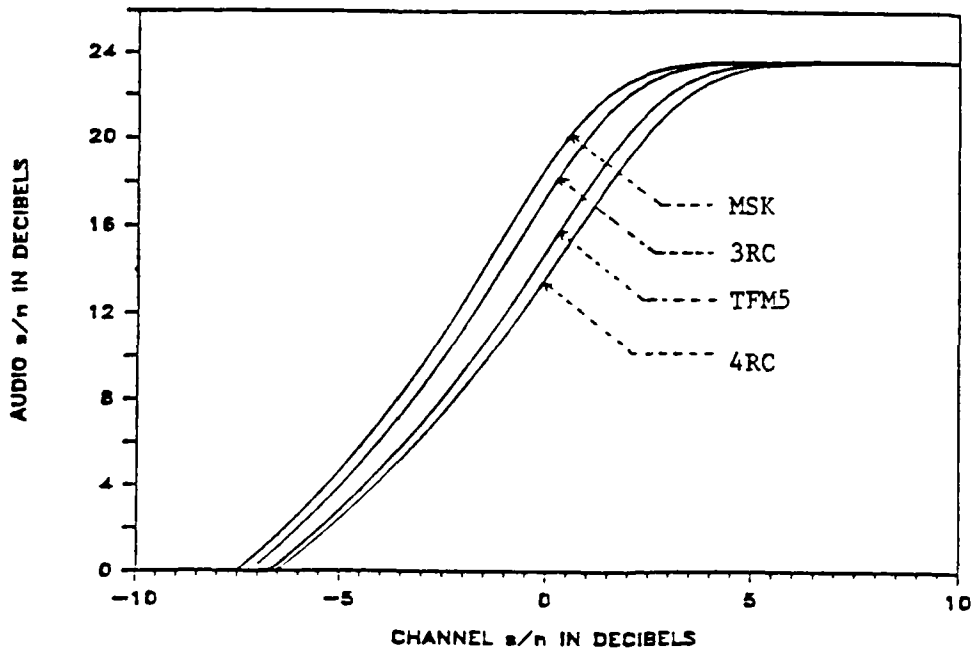


Figure 6.5 Performance of the speech transmission scheme for various modulation schemes in Rayleigh fading channel with 8 branch maximal ratio combining.

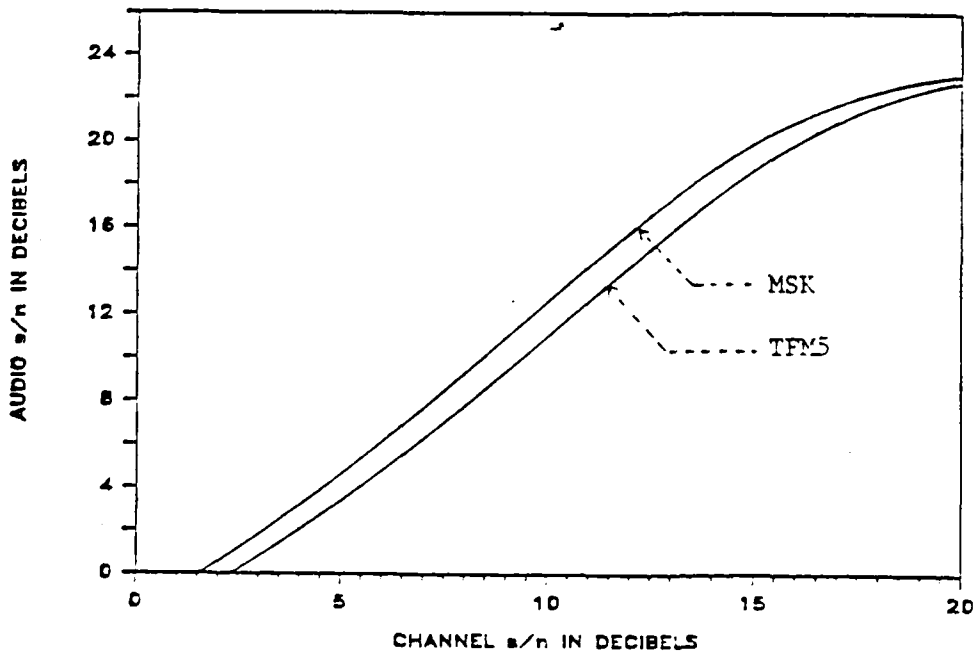


Figure 6.6 Performance of the speech transmission scheme for MSK and TFM5 modulation schemes in Rayleigh fading channel with 2 branch selection combining.

VII—PERFORMANCE DEGRADATION DUE TO RECEIVER MISMATCH IN BINARY CONTINUOUS—PHASE MODULATION SYSTEMS

Recently a great deal of attention has been focused on studying the performance of continuous-phase modulation (CPM) systems. CPM signals give constant envelope digital modulation schemes, which have the potential of both power and bandwidth efficiency under perfect synchronization conditions and complete knowledge of the channel.

Continuous-phase frequency shift keying (CPFSK) is a subclass of CPM where the instantaneous frequency is constant over each symbol interval and the phase is constrained to be continuous during the symbol transition. This constraint of continuous phase affects the signal in two ways:

- 1) Transients effects are lessened at the symbol transitions, thereby offering spectral bandwidth advantages [38]-[40].

- 2) Memory, imposed upon the waveform by continuous transitions, improves performance by providing for the use of several symbols to make a decision rather than the common approach of making independent symbol-by-symbol decisions.

This modulation has been investigated [41]-[45], and if the parameters of the modulation and demodulation are chosen correctly, binary CPFSK offers advantages in SNR over coherent PSK.

In all of these studies, the assumptions have been made that, a means is provided for establishing both, a perfect phase and bit

synchronization references, and the channel is AWGN with known power spectral density.

The objective of this chapter is to analyze the performance degradation of the CPFSK receivers under mismatch conditions. Closed form expressions for an upper bound on the BER in terms of amount of mismatch in time and phase are given.

This chapter is organized in three major sections. In the first section an introduction to CPFSK modulation scheme is given and then the optimum and suboptimum receivers are presented. In the final section the performance of the receivers under phase and time mismatch are derived and a brief discussion of the effect of different parameters on the performance degradation of the system is presented.

7.1 INTRODUCTION

CPFSK modulation schemes are subclass of the continuous phase modulation (CPM) signaling scheme where the instantaneous frequency is constant over each symbol interval. Thus, for a full response CPFSK systems the transmitted signal is

$$s(t, \underline{\alpha}) = \sqrt{\frac{2E}{T}} \cos(2\pi f_0 t + \phi(t, \underline{\alpha}) + \theta_0) ; \quad (7-1)$$

where the information carrying phase is

$$\phi(t, \underline{\alpha}) = \pi h \sum_{i=-\infty}^{\infty} \alpha_i (t - iT)/T ; \quad -\infty < t < \infty \quad (7-2)$$

is a continuous linear function of time t over each symbol interval and $\underline{\alpha} = \dots \alpha_2 \alpha_1 \alpha_0 \alpha_1 \dots$ is an infinity long sequence of uncorrelated M -ary data symbols, each taking one of the values

$$\alpha_i = \underline{+1}, \underline{+3}, \dots, \underline{+(M-1)} ; \quad i = 0, \underline{+1}, \underline{+2}, \dots \quad (7-3)$$

with equal probability $1/M$. (M is assumed even.)

E is the symbol energy, T is the symbol time, f_0 is the carrier frequency, θ_0 is an arbitrary constant phase shift.

The variable h is referred to as the modulation index, and as will be shown later, for implementation reasons, rational values of the modulation index are used. Fig.1 is a schematic modulator for CPM.

The signal is constructed such that two adjacent frequencies in the M -ary set are separated by h/T Hz. The possible phase

trajectories using the phase term

$$\alpha_i \pi h(t - iT)/T + \pi h \sum_{J=1}^{\ell-1} \alpha_J + \theta_0 \quad (7-4)$$

are shown in Fig.2, for binary modulation and $\theta_0 = 0$. As can be seen, the phase trajectories have a tree-like quality. Furthermore, if h is a rational number the tree will eventually fold on itself modulo 2π , producing a trellis like depiction.

Note that although the scheme is full response, the actual phase in any specific symbol interval depends upon the previous data symbols.

7.2 RECEIVER STRUCTURE

The CPFSK signal is assumed to be transmitted over an additive, white, and Gaussian noise (AWGN) channel having a one-sided noise power spectral density N_0 . Thus the signal available for observation is

$$r(t) = s(t, \underline{\alpha}) + n(t); \quad -\infty < t < \infty \quad (7-5)$$

where $n(t)$ is a Gaussian random process having zero mean and one-sided power spectral density N_0 . A detector which minimizes the probability of erroneous decision must observe the received signal $r(t)$ over the entire time axis and choose the infinitely long sequence $\hat{\underline{\alpha}}$ which minimizes the error probability. This is referred to as maximum likelihood sequence estimation (MLSE) [46].

By restricting the modulation indices to rational numbers, all CPM signals can be described as a finite state discrete time Markov processes. It is well-known [47] that the Viterbi algorithm (VA) is

a recursive optimal solution to the problem of estimating the state sequence of a discrete time finite state Markov process observed in memoryless noise. The complexity of the Viterbi receivers depends on the number of the states involved. From the performance view point it is difficult, if not impossible, to calculate the symbol error probabilities using the transfer function approach given by Viterbi [48]. This is because, first; the modulation is not linear, secondly the channel cannot be viewed as a discrete memoryless channel (DMC). Linearity makes it possible to choose a specific data sequence as a transmitted information sequence, hence we will have only one transfer function and the DMC makes it possible to use Hamming distances instead of the more general Euclidean distance in the general space.

To be able to study the performance of an optimum receiver for CPFSK systems, a suboptimum detector is studied instead. In the coherent case, this suboptimum detector observes the received signal $r(t)$ for N bit intervals to make decision about the first bit. In the noncoherent case the receiver will observe $2N+1$ bits of the CPFSK waveform and make decisions on the $n+1$ st (middle) bit the receiver shown in Fig.3 is derived in [43] for the coherent detection of CPFSK. The notation $s(t, \alpha_1, A_k)$ is used to represent the signal waveform during the observation interval, where A_k represents a particular data sequence (the tuple $\{\alpha_2, \alpha_3, \dots, \alpha_N\}$), and $k=1, 2, \dots, M$ where $M=2^{(N-1)}$.

Upper and lower bounds on the error probability are derived in the same reference, where it is shown that these bounds are tight at high SNR.

7.3 PERFORMANCE OF A MISMATCHED RECEIVER

The receiver shown in Fig. 7.3 computes the sums of random variables in the form

$$x_{1k} = \exp\left(\frac{2}{N_0} \int_0^{NT} r(t) s(t, 1, A_k) dt\right). \quad (7-6)$$

At low values of SNR the random variables x_{1k} can be approximated by

$$x_{1k} \approx 1 + \frac{2}{N_0} \int_0^{NT} r(t) s(t, 1, A_k) dt \quad (7-7)$$

Using the approximation of Eq.(7-7) the receiver operating at low SNR becomes,

$$\int_0^{NT} r(t) \left(\sum_{K=1}^M s(t, 1, A_k) \right) \stackrel{1}{\underset{-1}{\gtrless}} \int_0^{NT} r(t) \left(\sum_{K=1}^M s(t, -1, A_k) \right). \quad (7-8)$$

and the probability of bit error is given by

$$p = \sum_{J=1}^M \Pr(\text{error} \mid s(t, 1, A_j)) p(A_j). \quad (7-9)$$

At high SNR the union bound provides a tight upper bound. It can be shown that the probability of error for the receiver in Fig. 7.3 is overbounded by

$$p \leq \frac{1}{M} \sum_{\ell=1}^M \sum_{J=1}^M \Pr(x_{1\ell} < x_{-1j} \mid s(t, 1, A_\ell)), \quad (7-10)$$

where $x_{1\ell}$ is the output of the correlator matched to the signal $s(t, 1, A_\ell)$.

Case 1: Receivers Mismatched in Phase

At low SNR the decision variable, Λ , is a Gaussian random variable. The mean as a function of the phase error is derived in [49] and is given by

$$E\{\Lambda \mid s(t, 1, A_j)\} = \sum_{i=1}^N \mu_i \quad (7-11)$$

where

$$\mu_1 = E(\cos \phi - (\sin(2\pi h + \phi) - \sin \theta)/2\pi h) \quad (7-12)$$

$$\mu_i = E \cos^{i-2}(\pi h) \sin(\pi h) \left(\sin(\theta_i + \phi) + \sin(\theta_i + \pi h \alpha_i + \phi) \sin(\pi h \alpha_i)/2\pi h \alpha_i \right) \quad i = 2, 3, \dots, N \quad (7-13)$$

and

$$\theta_i = \sum_{j=1}^{i-1} \pi h \alpha_j \quad (7-14)$$

The variance of Λ is independent of ϕ and also is independent of a particular transmitted sequence and has the form

$$\text{Var}(\Lambda) = N_0 E \left(1 - \text{sinc}(2\pi h) + \frac{1}{2} \frac{(1 - \cos(2\pi h))(1 + \text{sinc}(2\pi h))(\cos^{2N-2}(\pi h) - 1)}{\cos^2(\pi h) - 1} \right) \quad (7-15)$$

The probability of error, given a particular transmitted sequence, is given by

$$\text{Pr}(\text{error} \mid s(t, 1, A_j)) = Q \left\{ \frac{E(\Lambda \mid s(t, 1, A_j))}{(\text{Var}(\Lambda))^{1/2}} \right\} \quad (7-16)$$

where

$$Q(x) = \int_x^{\infty} \frac{1}{\sqrt{2\pi}} \exp(-y^2/2) dy \quad (7-17)$$

In order to illustrate the effect of different values of the

phase mismatch on the behavior of the upper bound under low SNR conditions, Eq.(7-9) is evaluated and plotted for an observation interval of 5 bits and modulation index, h , of 0.715. These results are plotted in Fig. 4. The set of curves show that for $\text{SNR} < 6$ dB phase errors of less than 10° have small effects of the upper bound. The reason for restricting N to 5 bits is that it has been shown that increasing N beyond 5 will not improve the performance significantly. $h=0.715$ is the optimum value for the modulation index for binary CPFSK.

In order to compute Eq.(7-10), the statistics of the random variable $x_{1l} - x_{-1j}$ are needed. Again this random variable is Gaussian with mean value

$$E\{x_{1l} - x_{-1j} \mid s(t, 1, A_\ell)\} = E\left\{N \cos \phi - \sum_{i=1}^N \text{sinc}(\pi h(\alpha_i - \beta_i)/2) \cos\left(\sum_{j=1}^{i-1} \pi h(\alpha_j - \beta_j) + \frac{\pi h}{2}(\alpha_i - \beta_i) + \phi\right)\right\}, \quad (7-18)$$

where the α_i are the data bits A_1 , the β_i are the data bits A_j , and where $\alpha_1 = 1$ and $\beta_1 = -1$.

and variance

$$\text{Var}\{x_{1l} - x_{-1j} \mid s(t, 1, A_\ell)\} = NN_0 E(1 - \rho(\ell, j)), \quad (7-19)$$

where the correlation $\rho(\ell, j)$ can be written as

$$\rho(\ell, j) = \frac{1}{N} \sum_{k=1}^N \text{sinc}\left(\frac{\pi h}{2}(\alpha_k - \beta_k)\right) \cos\left(\frac{\pi h}{2}(\alpha_k - \beta_k) + \sum_{j=1}^{k-1} \pi h(\alpha_j - \beta_j)\right) \quad (7-20)$$

Further, the individual terms Eq.(7-10) are

$$\Pr(x_{1l} \leq x_{-1j} \mid s(t, 1, A_\ell)) = 0 \left\{ \frac{E\{x_{1l} - x_{-1j} \mid s(t, 1, A_\ell)\}}{\{\text{Var}\{x_{1l} - x_{-1j} \mid s(t, 1, A_\ell)\}\}^{1/2}} \right\} \quad (7-21)$$

The results are plotted in Fig.5. The plot shows that for high SNR a small mismatch in phase has a little effect on the upper bound, but larger errors $\phi > 20^\circ$ tend to degrade the performance of

the suboptimum receiver, as a matter of fact a mismatch of 20° at 8 dB SNR degrade the the upper bound by about 0.05 dB.

Case 2: Receivers Mismatched in Time

Following the same procedure, for a time error ΔT , Closed form expressions for the upper bound on the probability of bit error under low and high SNR can be derived (see [49]). The results are summarized in Fig.6-Fig.9. In these figures $\tau = \Delta T/T$. The fact that the results depend on the factor K , where $\omega_0 T = K$ is of no surprise, since higher K means larger carrier frequency for the same bit duration. The important conclusion at this point is that time errors affect the upper bounds more severely than phase errors do. for example when $K=2$, 5% error in timing degrades the upper bound at low SNR by about 2 dB and about 0.2 dB at high SNR. Increasing K has a severe effect on the upper bound for time errors $>10\%$. Note at 80 M b/s, 10% time error is equivalent to 1.25 nsec. The results emphasize the importance of time synchronization especially for channels which suffer time delay (e.g.; multipath channels, etc.).

7-4 CONCLUSION

The results demonstrate the various effects of phase and time mismatch at the receiver. The amount of degradation depends on the SNR range of interest. The often used assumption, $\omega_0 T = K$, (this assumption has been done in previous analysis of receiver performance [50]) is a critical assumption, and it is the responsibility of the designer to choose the minimum possible value of K , preferably $K=1$.

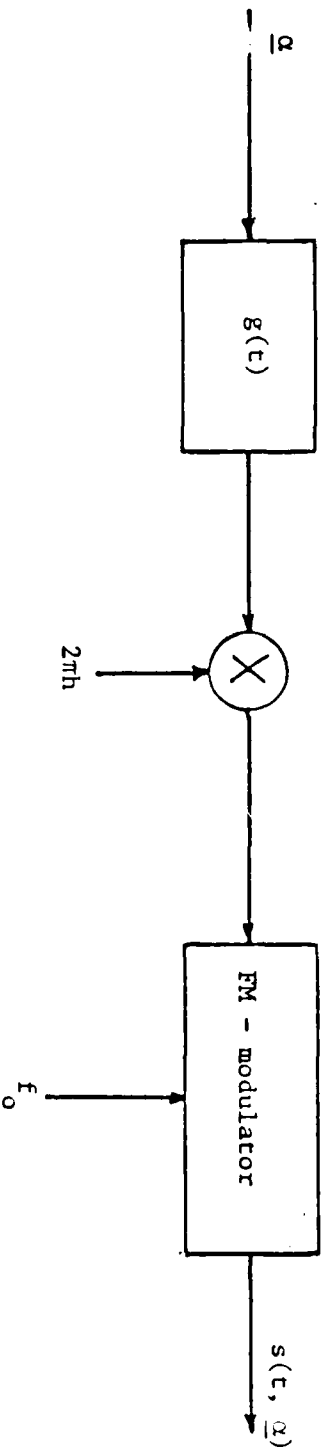


Figure 1. Schematic Modulator for CPM.

AD-A168 484

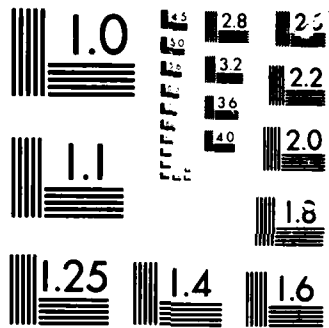
SPREAD SPECTRUM MOBILE RADIO COMMUNICATIONS(U) SOUTHERN 2/2
METHODIST UNIV DALLAS TEX DEPT OF ELECTRICAL
ENGINEERING S C GUPTA 31 MAR 86 AFOSR-TR-86-0323

UNCLASSIFIED

AFOSR-82-0309

F/B 17/2.1 NL





0000

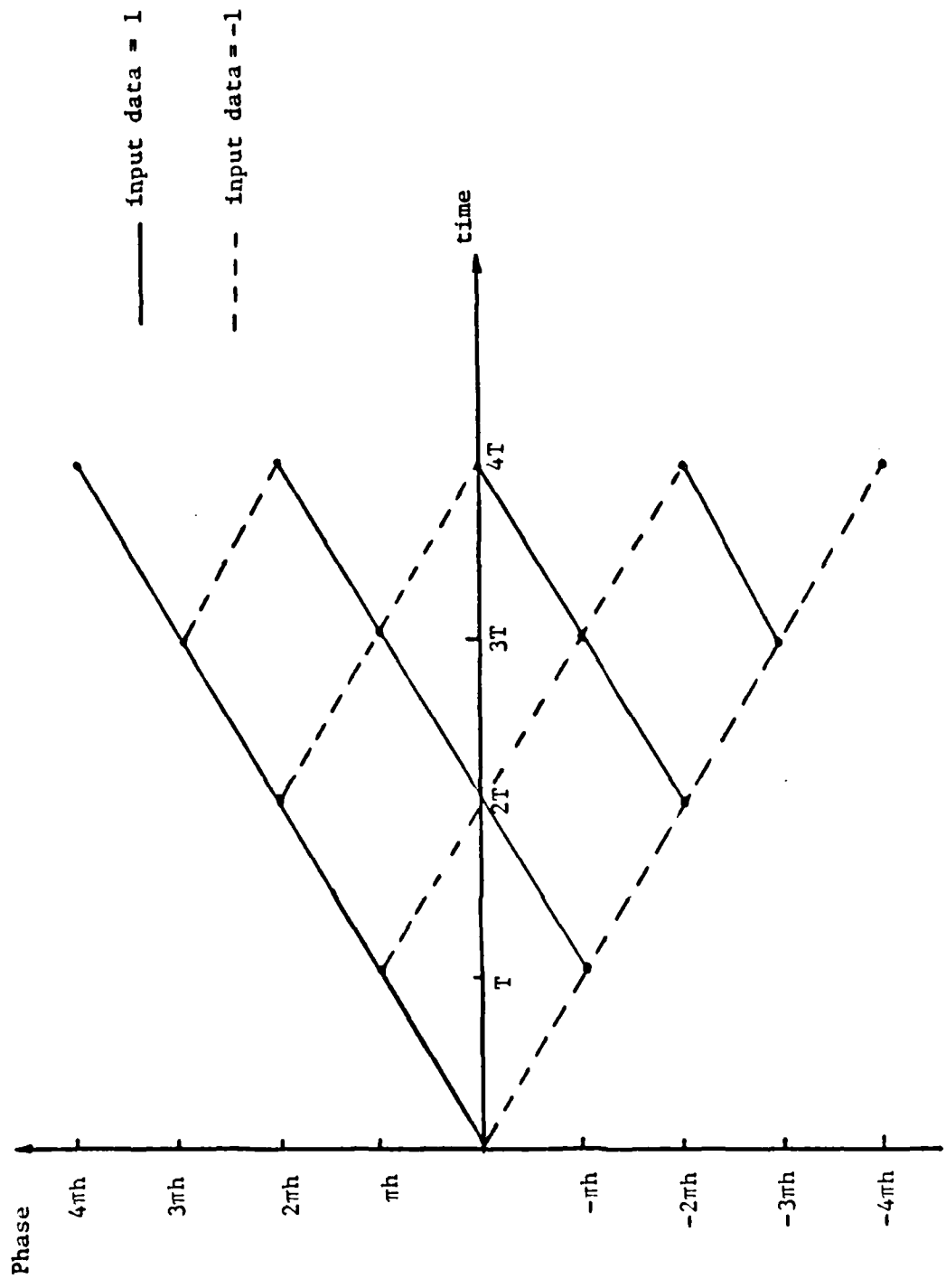


Figure 2. Phase trajectories for a binary full response CPFSK System.

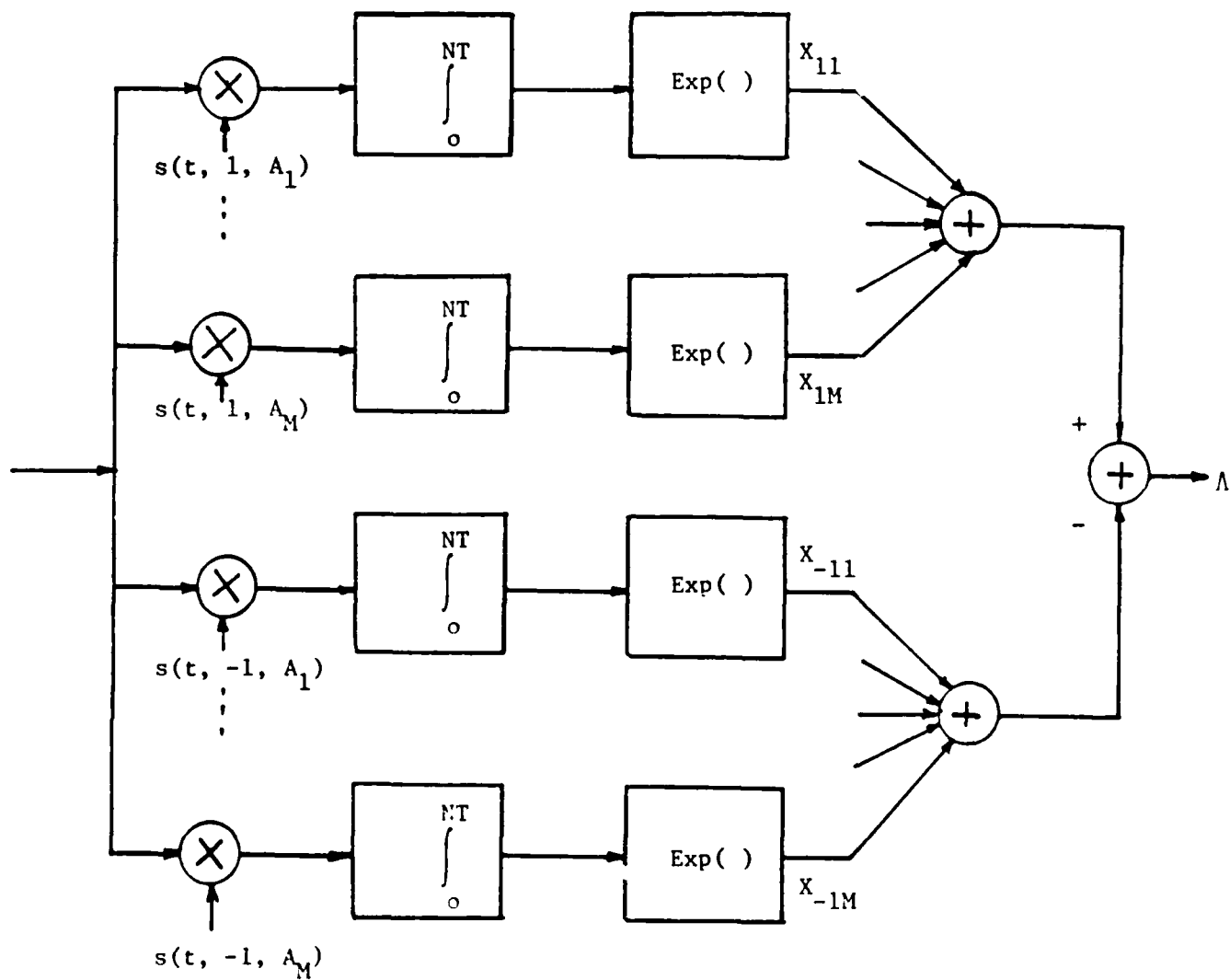


Figure 3. Block Diagram of Optimum Coherent Receiver.

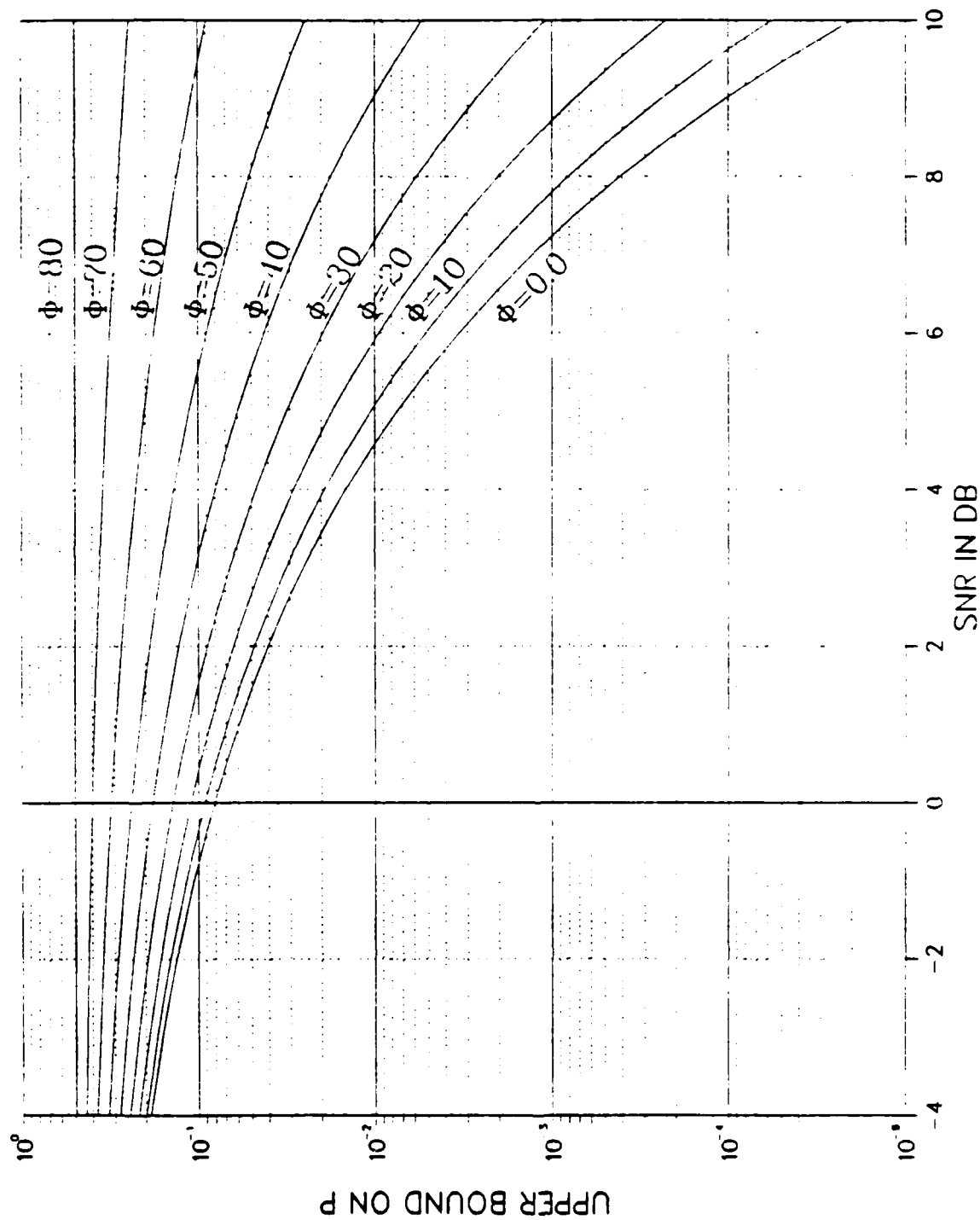


FIG.4 DEGRADATION IN PERFORMANCE DUE TO PHASE ERRORS
(LOW SNR)

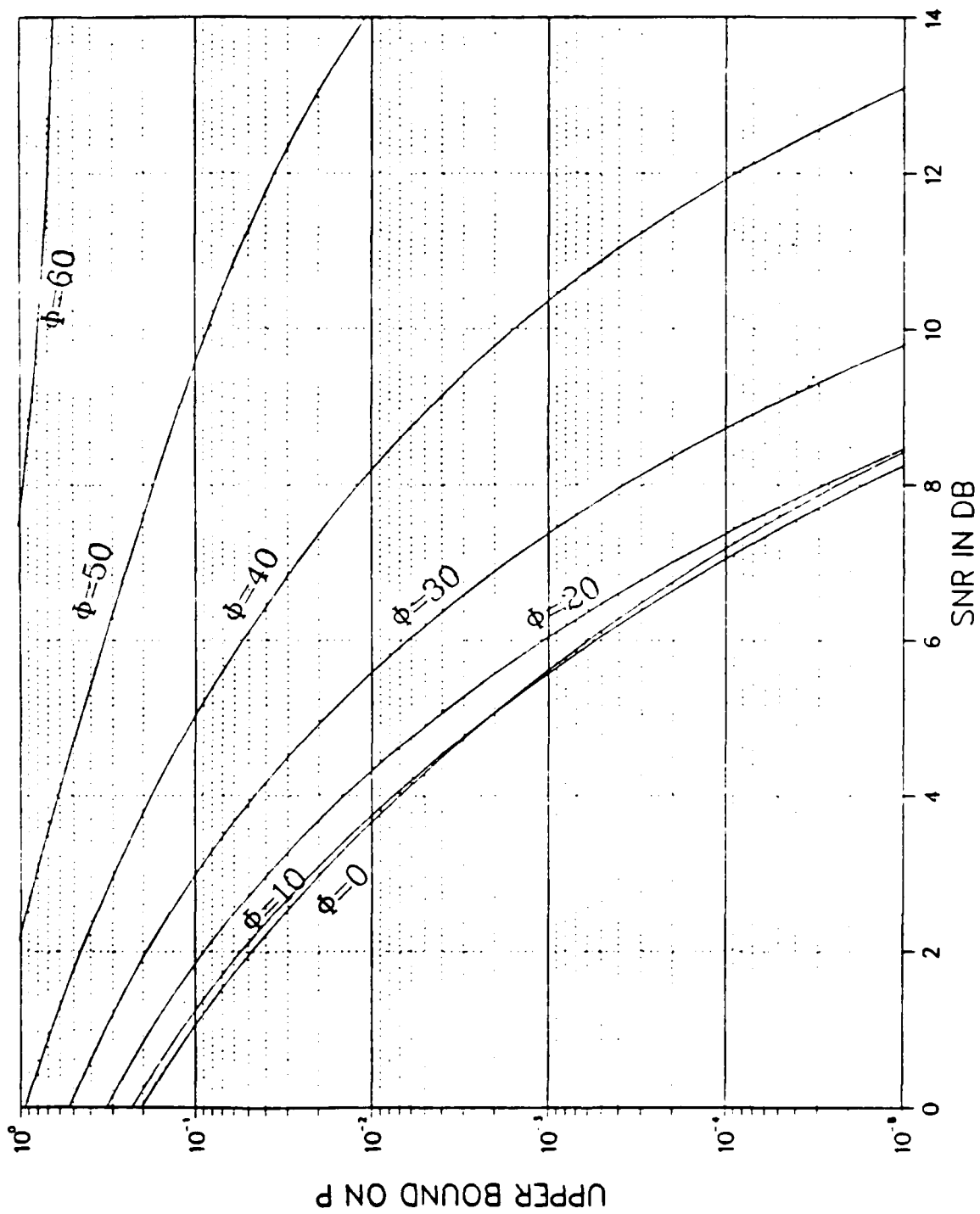


FIG.5 DEGRADATION IN PERFORMANCE DUE TO PHASE ERRORS
(HIGH SNR)

$K=1$

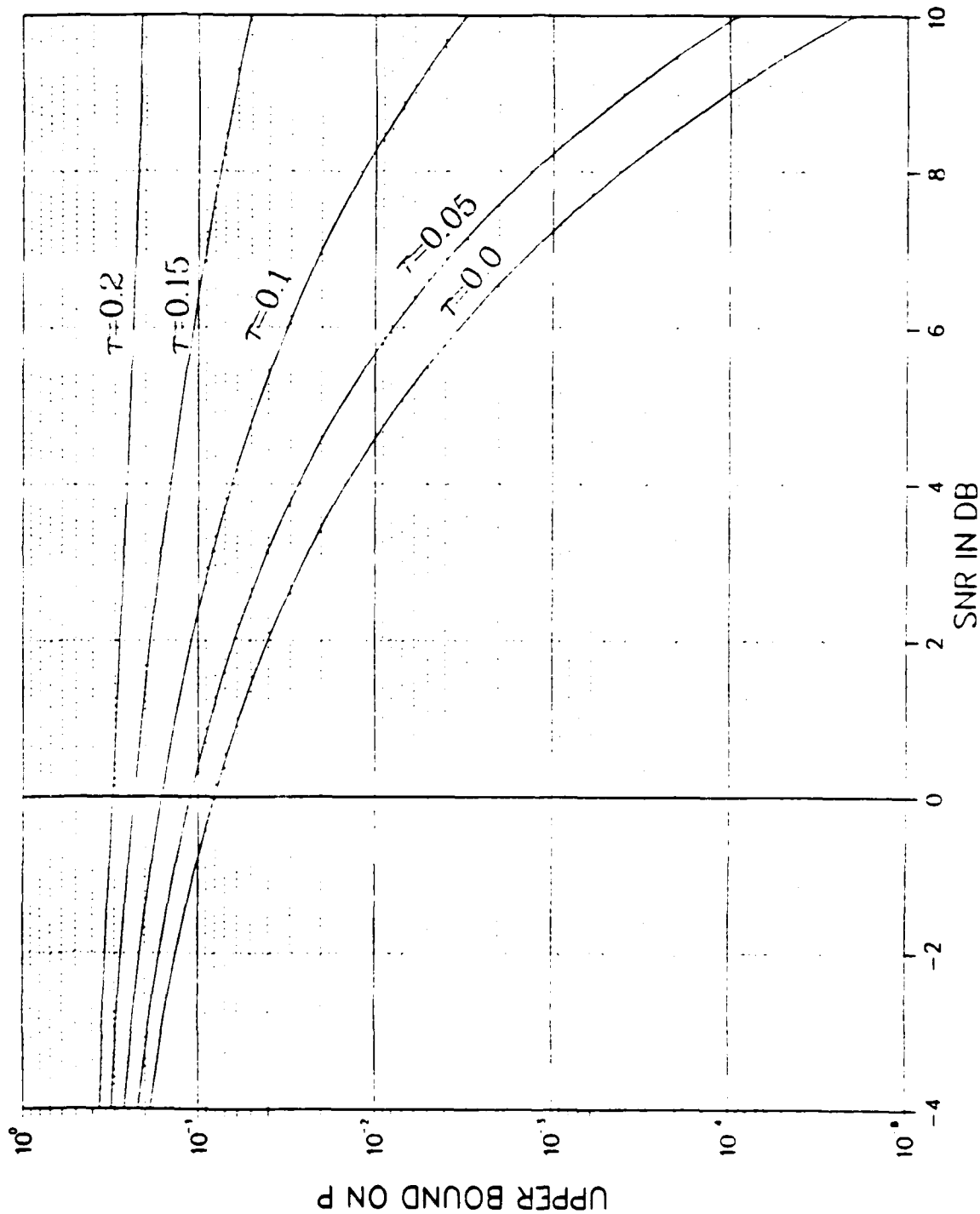


FIG.6 DEGRADATION IN PERFORMANCE DUE TO TIME ERRORS
(LOW SNR)

$K=2$

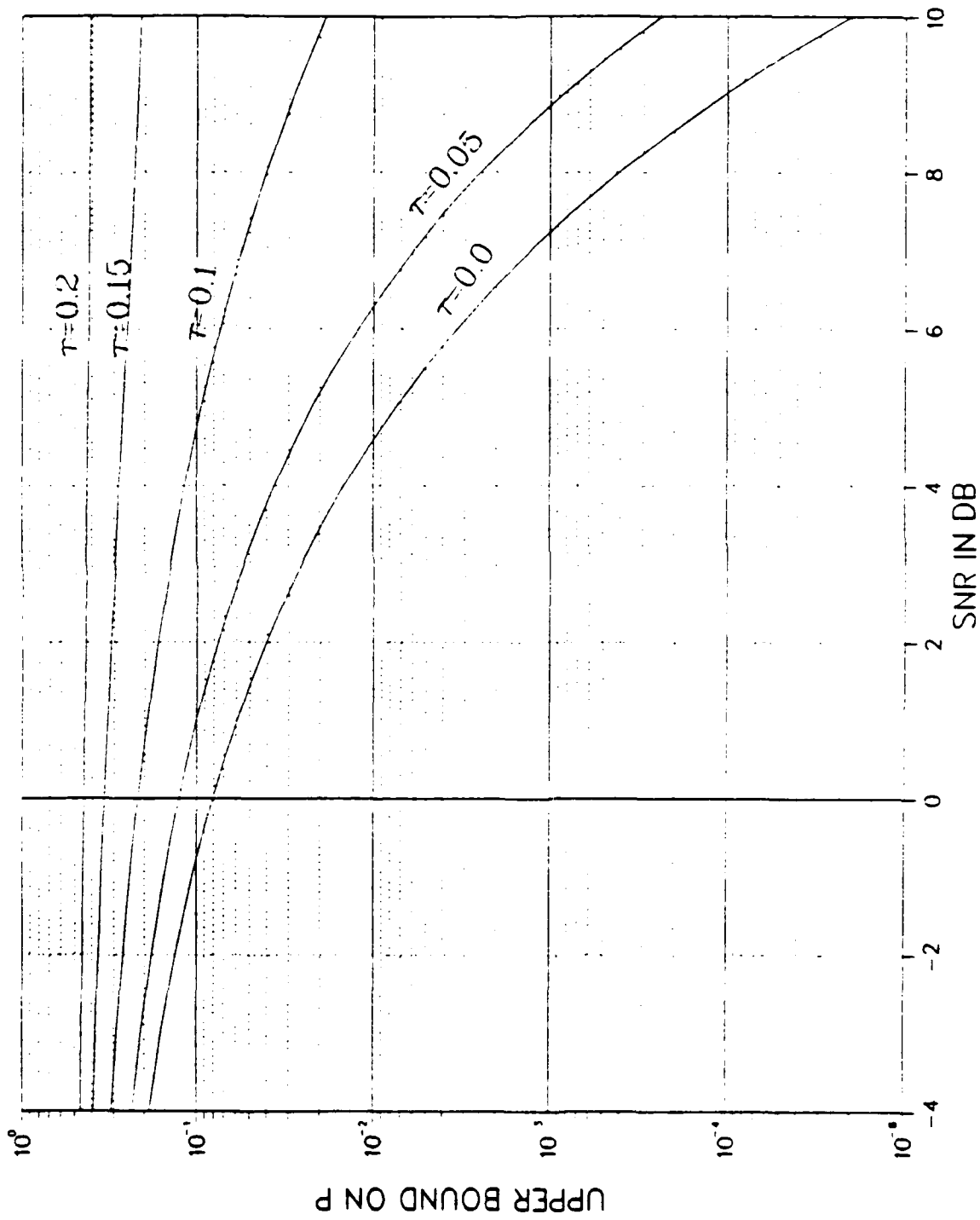


FIG. 7.7 DEGRADATION IN PERFORMANCE DUE TO TIME ERRORS
(LOW SNR)

$K=1$

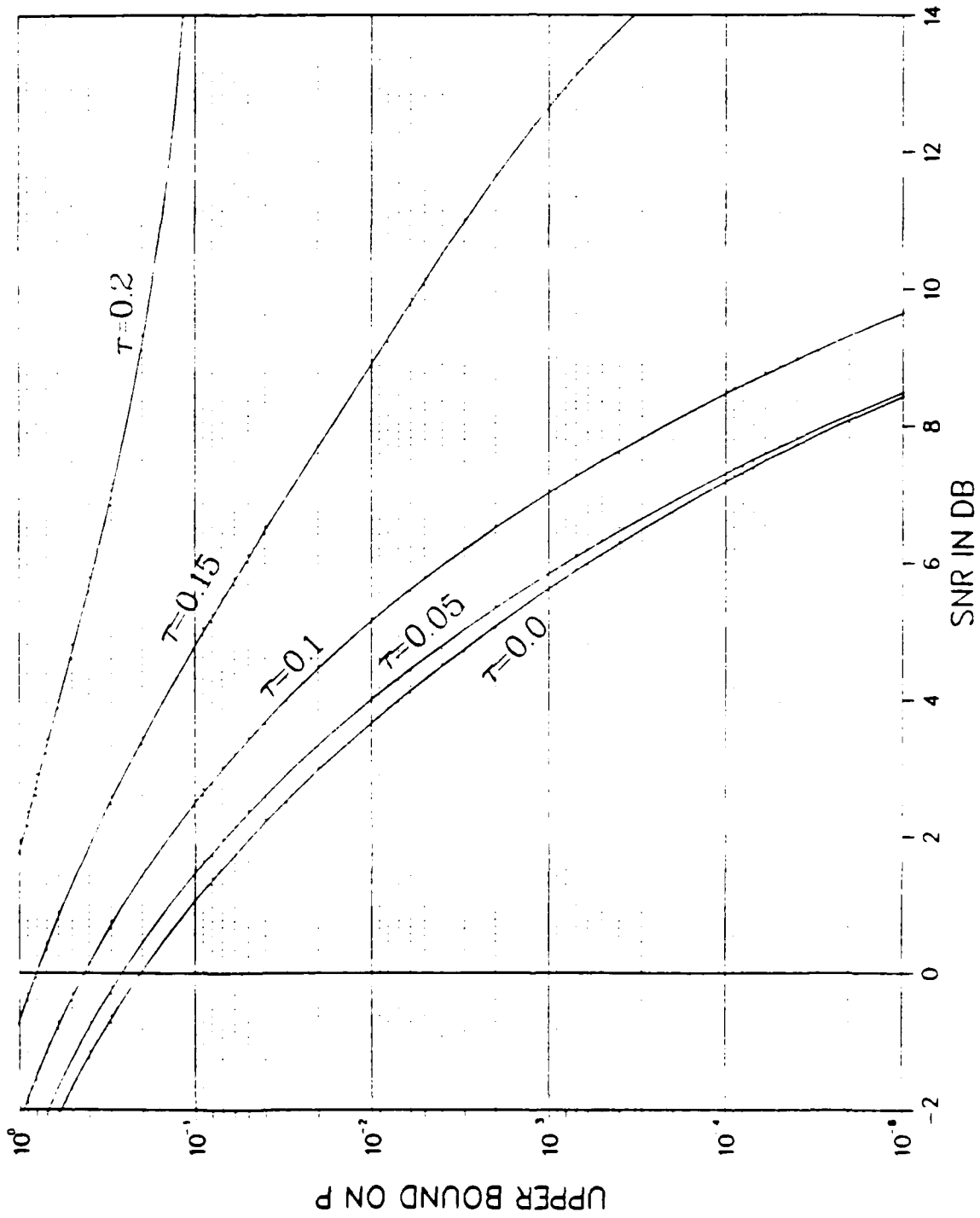


FIG.8 DEGRADATION IN PERFORMANCE DUE TO TIME ERRORS
(HIGH SNR)

$K=2$

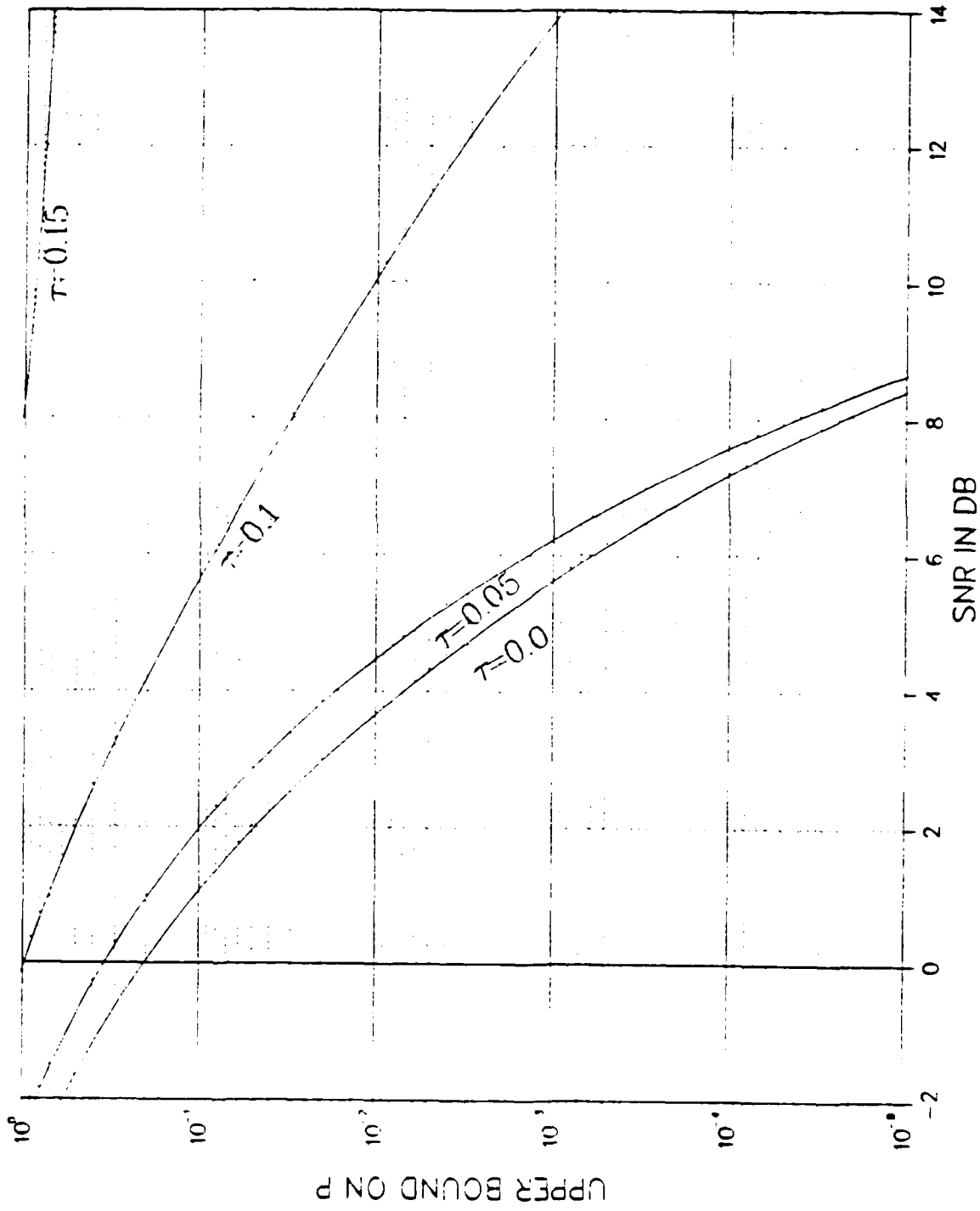


FIG.9 DEGRADATION IN PERFORMANCE DUE TO TIME ERRORS
(HIGH SNR)

REFERENCES

- [1] John M. McQuillan and Vinton G. Cerf, Tutorial: A Practical View of Computer Communications Protocols, IEEE Computer Society, IEEE Catalog No. EHO 137-0, 1978.
- [2] Pall Spilling and Earl Craighill, "Digital Voice Communications in the Packet Radio Network", Proceedings of the International Conference on Communication, 1980.
- [3] L. Kleinrock and F.A. Tobagi, "Packet Switching in Radio Channels: Part I - Carrier Sense Multiple-Access Modes and Their Throughput - Delay Characteristics", IEEE Transactions on Communications, Vol. COM-23, No. 12, December 1975, pp. 1400-1416.
- [4] F.A. Tobagi, "Multi-Access Protocols in Packet Communication Systems," IEEE Transactions on Communications, Vol. COM-28, No. 4, April 1980, pp. 468-488.
- [5] W.C. Jakes, "Microwave Mobile Communications," John Wiley, 1974.
- [6] Robert E. Kahn, "The Organization of Computer Resources into a Packet Radio Network," IEEE Transactions on Communications, Vol. COM-25, No. 1, January 1977, pp. 169-178.
- [7] J.S. DaSilva, H.M. Hafez, and S.A. Mahmoud, "Optimal Packet Length for Fading Land-Mobile Data Channels," Proceedings of the International Conference on Communications, 1980.
- [8] Wesley W. Chu, "Optimal Message Block Size for Computer Communications with Error Detection and Retransmission Strategies," IEEE Transactions on Communication, vol. COM-22, No. 10, pp. 1516-1525, October 1974.
- [9] Leonard Kleinrock and F.A. Tobagi, "Random Access Techniques for Data Transmission over Packet Switched Radio Channels," National Computer Conference, AFIPS Conf. Proc., Vol. 44, AFIPS Press, 1975, pp. 187-201.
- [10] Mischa Schwartz, "Computer-Communication Network Design and Analysis," Englewood Cliffs, N.J., Prentice Hall, 1977.
- [11] M. Schwartz, W. Bennett, and S. Stein, "Communication Systems and Techniques," New York, McGraw Hill, 1966.
- [12] M. Abramowitz and I.A. Stegun, "Handbook of Mathematical Functions," (Applied Mathematics Series 55), Washington D.C., National Bureau of Standards, 1964.
- [13] J. Riordan, "Combinational Identities," New York, Interscience, 1968.
- [14] L.B.W. Jolley, "Summation of Series," New York, Dover, 1961.

- [15] Nakagami M., "The m -Distribution - A General Formula of Intensity Distribution of Rapid Fading," Statistical Methods in Radio Wave Propagation, W.C. Hoffman (ed.), pp. 3-36, Oxford, Pergamon, 1960.
- [16] M. Schwartz, W. Bennett and S. Stein, "Communication Systems and Techniques", N.Y., McGraw-Hill, 1966.
- [17] Leonard Kleinrock and F.A. Tobagi, "Packet Switching in Radio Channels: part II - The Hidden Terminal Problem in Carrier Sense Multiple-Access and the Busy-Tone Solution," IEEE Trans. on Commun., vol. COM-23, No. 12, pp. 1417-1433, December 1975.
- [18] Rajeev Sinha and S.C. Gupta, "Carrier Sense Multiple Access for Mobile Packet Radio Channels: Performance Evaluation", Proceedings of the Eighteenth Annual Conference on Information Sciences and Systems, March 1984, Princeton University.
- [19] Kazuaki Murota and Kenkichi Hirade, "GMSK Modulation for Digital Mobile Radio Telephony", IEEE Trans. on Commun., Vol. COM-29, No. 7, July 1981, pp. 1044-1050.
- [20] W.C. Lee, "Mobile Communication Engineering", McGraw-Hill, Inc., 1982.
- [21] G.R. Cooper and R.W. Nettleton, "A Spread-Spectrum Technique for High-Capacity Mobile Communications," IEEE Transactions on Vehicular Technology, Vol. VT-27, No. 4, November 1978, pp. 264-275.
- [22] F.A. Tobagi and V. Bruce Hunt, "Performance Analysis of Carrier Sense Multiple Access with Collision Detection," Computer Networks 4 (1980) 245-259, North-Holland Publishing Company.
- [23] F. Hansen and F.I. Meno, "Mobile Fading-Rayleigh and Lognormal Superimposed," IEEE Transactions on Vehicular Technology, Vol. VT-20, No. 4, November 1977, pp. 332-335.
- [24] A.J. Viterbi and I.M. Jacobs, "Advances in Coding and Modulation for Noncoherent Channels Affected by Fading, Partial-Band and Multiple-Access Interference," Advances in Communication Systems, Vol. 4, A.J. Viterbi, Ed., Academic Press, New York (1975).
- [25] F.A. Tobagi and L. Kleinrock, "Packet Switching in Radio Channels: Part IV - Stability Considerations and Dynamic Control in Carrier Sense Multiple Access," IEEE Transactions on Communications, Vol. COM-25, pp. 1103-1120, October 1977.
- [26] N.F. Maxemchuk, "A Variation on CSMA/CD that yields Movable TDM Slots in Integrated Voice/Data Local Networks," The Bell System Technical Journal, Vol. 61, No. 7, September 1982, pp. 1527-1550.
- [27] T. Aulin and C.E. Sundberg, "Continuous Phase Modulation - Part I: Full Response Signaling," IEEE Trans. Commun., COM-29, No. 3 (March 1981), pp. 196-209.

- [28] T. Aulin, N. Rydbeck, and C.E. Sundberg, "Continuous Phase Modulation - Part II: Partial Response Signaling," IEEE Trans. Commun., COM-29, No. 3 (March, 1981), pp. 210-225.
- [29] T. Aulin, C.E. Sundberg, and A. Svensson, "MSK-Type Receivers for Partial Response Continuous Phase Modulation," Int. Conf. Commun., Philadelphia Pennsylvania, June 1982, pp. 6F3.1-6.
- [30] R. deBuda, "Coherent Demodulation of Frequency-Shift Keying with Low Deviation Ratio," IEEE Trans. Commun., COM-20 (June 1972), pp. 429-435.
- [31] A. Sevensson and C.E. Sundberg, "Optimum MSK-type Receivers for CPM on Gaussian and Rayleigh Fading Channels," IEEE Proceedings, Vol. 131, Pt. F, No. 5, August 1984. pp. 480-490.
- [32] Vijay Varma and S.C. Gupta, "Performance of Partial Response Continuous Phase Modulation in the Presence of Adjacent Channel Interference and Gaussian Noise," Submitted to Fifth Annual Phoenix Conference on Computers and Communications, March 1986.
- [33] C.E. Sundberg, "Error Probability of Partial Response Continuous Phase Modulation with Coherent MSK-Type Receiver, Diversity and Slow Rayleigh Fading in Gaussian Noise," B.S.T.J., 61, October 1982, pp. 1933-1963.
- [34] P.S. Henry and B.S. Glance, "A New Approach to High Capacity Digital Mobile Radio," B.S.T.J., 60, No. 8 (October 1981), pp. 1891-1904.
- [35] Y.S. Yeh and D.O. Reudink, "Efficient Spectrum Utilization for Mobile Radio Systems Using Space Diversity," IEEE Trans. Commun., COM-30, No. 3 (March 1982), pp. 447-455.
- [36] D.J. Goodman and C.E. Sundberg, "Transmission Errors and Forward Error Correction in Embedded Differential Pulse Code Modulation," B.S.T.J., 62, November, 1983, pp. 2735-2764.
- [37] D.J. Goodman and C.E. Sundberg, "Combined Source and Channel Coding for Variable Bit Rate Speech Transmission," B.S.T.J., 62, Sept., 1983, pp. 2017-2036.
- [38] W.K. Bennett and S.O. Rice, "Spectral Density and Autocorrelation Functions Associated with Binary Frequency Shift Keying," BSTJ, Vol. 42, pp. 2355-2385, Sept. 1963.
- [39] R.R. Anderson and J. Salz, "Spectra of Digital FM," BSTJ, Vol. 44, pp. 1165-1189, July/August 1965.
- [40] M.G. Pelchat, "The Autocorrelation Function and Power Spectrum of PCM/FM with Random Binary Modulating Waveforms," IEEE Trans. Space Electron. Telem., pp. 39-44, March 1964.
- [41] T. Aulin and C.E. Sundberg, "Continuous Phase Modulation - Part I: Full Response Signaling," IEEE Trans. Commun., Vol. COM-29, No. 3, pp. 196-209, March 1981.

- [42] M.G. Pelchat, R.C. Davis, and M.B. Luntz, "Coherent Demodulation of Continuous Phase Binary FSK Signals," in Proc. Int. Telemetry Conf., pp. 181-190, Washington, DC 1971.
- [43] W.P. Osborne and M.B. Luntz, "Coherent and Noncoherent Detection of CPFSK," IEEE Trans. Commun., Vol. COM-22, No. 87, pp. 1023-1036, Aug. 1974.
- [44] T.A. Schonhoff, "Symbol Error Probabilities for M-ary CPFSK: Coherent and Noncoherent Detection," IEEE Trans. Commun., Vol. COM-24, No. 6, pp. 664-652, June 1976.
- [45] _____, "Bandwidth vs. Performance Considerations for CPFSK," IEEE National Telecommunications Conference, New Orleans, 1975.
- [46] T.A. Schonhoff, H.E. Nichols, and H.M. Gibbons, "Use of the MLSE Algorithm to Demodulate CPFSK," in Proc. Int. Conf. Commun., pp. 25.4.1-25.4.5, Toronto, Canada 1978.
- [47] G.D. Forney, "The Viterbi Algorithm," Proc. of the IEEE, Vol. 61, No. 3, pp. 268-277, March 1973.
- [48] A.J. Viterbi and J.K. Omura, Principles of Digital Communication and Coding, New York: McGraw-Hill, 1979.
- [49] S.S. Soliman, "Performance Degradation Due to Receiver Mismatch in CPFSK Systems," submitted to Phoenix Conference on Computer and Communication 1985.
- [50] M.K. Simon and C.C. Wang, "Bit Synchronization of Differentially Detected MSK and GMSK," in Proc. of Int. Con. Commun. pp. 18.7.1-18.7.8, Chicago, Illinois, June 1985.

END

DOTIC

8-86